ANALYSIS OF AN A.C. TACHOMETER USED AS AN ACCELEROMETER

EDWARD M. BATY
AND
THOMAS M. WARD, JR.

ANALYSIS OF AN A.C. [illegible]

[illegible]

by

ADAM M. BATY, LIEUTENANT, U.S.N.
B.S.(C.E.), Iowa State College, 1950
B.S.(E.E.), United States Naval Postgraduate School, 1957

THOMAS F. HARD, JR. LIEUTENANT, U.S.N.
B.S. United States Naval Academy, 1951
B.S.(E.E.), United States Naval Postgraduate School, 1957

SUBMITTED IN PARTIAL FULFILLMENT OF THE

REQUIREMENTS FOR THE DEGREE OF

MASTER OF SCIENCE

at the

MASSACHUSETTS INSTITUTE OF TECHNOLOGY

1958

ANALYSIS OF AN A.C. TACHOMETER USED AS AN ACCELEROMETER

by

Edward M. Baty
Thomas M. Ward, Jr.

Submitted to the Department of Aeronautical Engineering on May 26, 1958, in partial fulfillment of the requirements for the degree of Master of Science.

ABSTRACT

Various writers have stated that an alternating current tachometer generator has a voltage output proportional to the shaft angular acceleration, when excited with direct current.

This thesis deals with the derivation of a performance equation relating the voltage output to the shaft angular acceleration and an experimental and computer verification of the derived equation. It was found that the voltage output is proportional to the shaft angular acceleration modified by a deviation function. The deviation function is a function of the type of shaft motion to which the instrument is subjected and in general decreases the proportionality with increasing shaft angular velocity.

Thesis Supervisor: Robert K. Mueller
Title: Associate Professor of Aeronautical Engineering

Thesis Supervisor: Richard H. Frazier
Title: Associate Professor of Electrical Engineering

ACKNOWLEDGMENT

The authors express their appreciation to the Servomechanisms Laboratory, Massachussetts Institute of Technology, for the use of their sine-drive; to Mr. John Barley for his help in setting up some of the experimentation; to Mr. Daniel Goldenberg for his mathematical assistance; to Mrs. Bette Baty for the typing of this thesis; to our wives for their patience; and to Dr. Robert K. Mueller and Prof. Richard H. Frazier for their advice and guidance as thesis supervisors.

TABLE OF CONTENTS

OBJECT

The object of this thesis is to analyze an a-c drag-cup tachometer, that is excited with a-c, to determine the performance equation relating voltage output to shaft acceleration. This analysis is to verify or establish limitations on the use of this instrument as an angular accelerometer.

CHAPTER I

INTRODUCTION

Several authors, notably Ahrendt [1]* and Davis [2], have stated that it is possible to excite an induction tachometer with d-c and obtain a d-c output voltage proportional to the shaft angular acceleration. When the excitation is d-c, the quadrature flux along the secondary (output) axis will also be d-c with a density proportional to the speed of the rotor. With the rotor shaft at constant speed, the flux along the output axis will be steady and will not generate an output voltage. However, as the velocity changes (acceleration) the output axis windings will detect the rate of change of flux and produce a d-c output voltage proportional to the acceleration of the shaft.

This differs from the normal application of an induction tachometer where the excitation is a-c and the output voltage is a-c with an amplitude proportional to the velocity of the shaft.

Fowle [3] and Lovett [4] have sucessfully used this application of a d-c excited induction tachometer in a servo loop as the source of a feedback signal proportional to acceleration. The use of acceleration damping in servomechanisms is analogous to inertia, similar to velocity damping being analogous to viscous drag. By proper adjust-

*The numbers in parentheses refer to the references in the Bibliography.

ment of the acceleration damping, a "negative inertia" can be designed into a system for increasing speed of response.

Fowle and Lovett determined the angular acceleration-output voltage sensitivity of the tachometer experimentally and used a proportionality constant to represent the relationship.

The purpose of this thesis is to verify or establish limitations of the use of a proportionality constant to represent the performance equation of the induction tachometer when used as an accelerometer.

CHAPTER 2

ANALYSIS

Description of Tachometer Considered

The analysis is made on a drag-cup induction tachometer (induction generator). Due to the availability of the unit itself and to information as to its physical properties[7][8] an ARMA 1B400 INDUCTION GENERATOR is used. This is a four pole drag-cup induction generator with concentrated windings wound on a stationary laminated stator core. The magnetic path is completed through a laminated stator in the generator case. There are two sets of windings on the core located in electrical quadrature. The normal excitation when used as a tachometer is 115 volts 400 cps in series with a standard input network.

The analysis is made considering a two pole device for simplicity, with notations made when the analysis is applied to the particular four pole tachometer used.

Fig. A-1 shows the physical dimensions of the ARMA 1B400 and the description of the dimensions used in the analysis.

Assumptions used

The analysis is based on the following assumptions:

1. The main (input) winding is excited with direct current from a constant current source.
2. The main winding flux, Φ_m, is of constant value, evenly distributed around the periphery

of the center core thus creating a constant flux density, normal to the surface of the core and cup. Effects of winding slots on this distribution are neglected.

3. Due to the high permeability of the iron structure, all the magnetic potential drop is assumed to occur across the air gap.
4. There is negligible leakage flux due to rotor (cup) currents. The leakage flux in the main windings is also neglected due to the assumption of d-c excitation with a constant current source.
5. The output winding is operating effectively open circuit. This can be practically realized in actual use, so that there is no effect due to current in the output windings.

Derivation of Performance Equation

In this derivation the Practical Unit System [6] will be used. This is an adaption of the CGS Electromagnetic Unit System using volts, amperes, and ohms.

Fig. 2-1 shows the representations and symbols used in this derivation.

$$\phi_A = \phi_m - \phi_x$$

$$= \frac{4\pi}{10}\left(\frac{N_m i_m}{\mathcal{R}} - \frac{\mathcal{F}_x}{\mathcal{R}}\right)$$

$$= \frac{4\pi}{10\mathcal{R}}\left(N_m i_m - i_x\right) \quad \text{Maxwells (1)}$$

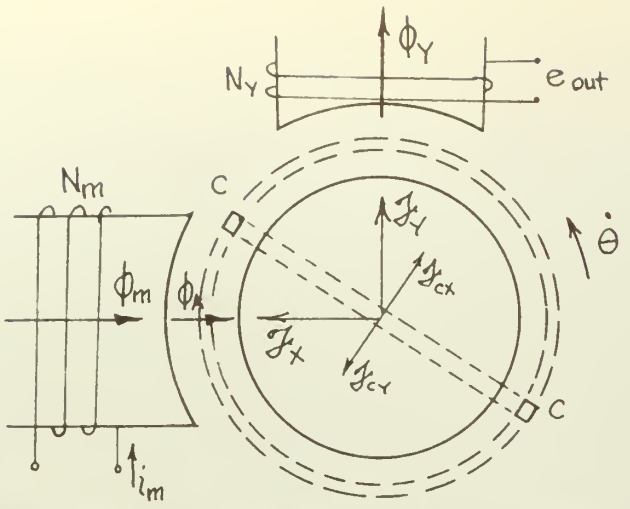

N_m Number of turns on the main (X or input) winding.

N_y Number of turns on the Y (output) axis winding.

ϕ_m Flux developed from the main winding turns.

ϕ_A Resultant flux in the air gap, along the X-axis.

ϕ_Y Flux along the Y-axis.

$\mathcal{F}_{cx}, \mathcal{F}_{cy}$ Representations of the instantaneous mmf's produced by current flowing in a single coil (c-c) which represents an element of the drag-cup. The x and y subscripts designates the flux cut by the coil to produce the current. All the current produced by cutting ϕ_A is symmetrical about the Y-axis and all the current produced by cutting ϕ_Y is symmetrical about the Y-axis.

$\mathcal{F}_X, \mathcal{F}_Y$ Representations of the resultant mmf's created by the currents in the drag-cup symmetrical about their respective axes.

Fig. 2-1. Representation and definitions of the flux and mmf symbols.

where $\mathcal{R}$ is the reluctance of the magnetic path, and since all the reluctance is considered to be concentrated in the air gap,

$$\mathcal{R} = \frac{2(\text{gap length})}{(\text{area})} \qquad \text{centimeters}^{-1}$$

Also, i_x is the resultant current in a single coil equivalent of the drag-cup to produce $\mathcal{F}_A$. i_x is symmetrical about the X axis. Similarly, i_y is the resultant current, symmetrical about the Y axis, which would flow in a single coil equivalent to produce $\mathcal{F}_Y$. Therefore

$$\phi_Y = \frac{4\pi}{10}\frac{\mathcal{F}_Y}{\mathcal{R}} = \frac{4\pi}{10\mathcal{R}}\, i_y \qquad (2)$$

and

$$B_A = \frac{\phi_A}{(\text{area})} = \frac{4\pi}{10}\,\frac{(N_m i_m - i_x)}{(\text{area})(2\,\text{gap})/(\text{area})}$$

$$= \frac{4\pi(N_m i_m - i_x)}{10\,(2g)} \qquad \text{gauss} \qquad (3)$$

also

$$B_Y = \frac{4\pi}{10(2g)}\, i_y \qquad (4)$$

Now using the assumption of square wave distribution of flux on the pole faces, the induced emf's due to rotation of the cup are:

$$e^{*}_{SA} = \frac{1}{10^8}\, 2 B_A l r \dot{\theta} \qquad \text{volts} \qquad (5)$$

$$e_{SY} = \frac{1}{10^8}\, 2 B_Y l r \dot{\theta} \qquad (6)$$

*See Appendix A, Eq. A-4

where e_{sA} and e_{sY} are the speed voltages due to cutting B_A and B_Y respectively, ℓ is the axial length of the pole face, r is the radius to the center of the cup shell, and $\dot{\theta}$ is the speed of rotation of the drag-cup expressed in mechanical radians per second.

Again considering the drag-cup as an equivalent single coil

$$L\frac{di_y}{dt} + Ri_y = e_{sA} \tag{7}$$

$$L\frac{di_x}{dt} + Ri_x = e_{sY} \tag{8}$$

where R* and L** are the resistance and inductance of the drag-cup when it is considered as an equivalent single coil.

Substituting Eqs. (3), (4), (5), and (6) into (7) and (8).

$$L\frac{di_y}{dt} + Ri_y = \left(\frac{4\pi}{10^9}\right)\left(\frac{\ell r}{g}\right)\dot{\theta}\left(N_m i_m - i_x\right) \tag{9}$$

$$L\frac{di_x}{dt} + Ri_x = \left(\frac{4\pi}{10^9}\right)\left(\frac{\ell r}{g}\right)\dot{\theta}\, i_y \tag{10}$$

or

$$L\frac{di_y}{dt} + Ri_y = K\dot{\theta}\left(N_m i_m - i_x\right) \tag{11}$$

$$L\frac{di_x}{dt} + Ri_x = K\dot{\theta}\, i_y \tag{12}$$

where

$$K = \left(\frac{4\pi}{10^7}\right)\left(\frac{\ell r}{g}\right) \tag{13}$$

Eqs. (11) and (12) represent one method of explaining the actions of a drag-cup induction generator. First, the

*See Appendix A, Eq. A-4
**See Appendix B, Eq. B-6

incremental coils of the cup cut the main field flux, ϕ_m, and voltages are induced in all the increments. The induced voltage causes a distribution of current in the cup which is symmetrical about the Y-axis, and iy is the equivalent current in a single coil, symmetrical about the Y-axis, that would produce the same cross-axis flux, ϕ_Y, as would be produced by the summation of all the currents in the incremental coils. The cup will also be cutting this cross-axis flux and this will induce voltages in all the increments which will create a current distribution symmetrical about the Y-axis. This produces an mmf along the X-axis, $\mathcal{F}_y$, which opposes the main field flux and is therefore a demagnetizing force.

Therefore by solving Eqs. (11) and (12) for i_y, a time dependent equation for the current along the Y-axis can be obtained. i_y is proportional to the magnitude of the Y-axis flux and therefore the first derivative of i_y is proportional to the rate of change of flux along the Y-axis.

From the rate of change of flux along the Y-axis the output voltage can be obtained.

Solving Eq. (9) for i_x

$$i_x = N_m i_m - \frac{L}{K\dot{\theta}} \frac{di_y}{dt} - \frac{R}{K\dot{\theta}} i_y \qquad (14)$$

then

$$\frac{di_x}{dt} = -\frac{L}{K}\left(\frac{1}{\dot{\theta}} \frac{d^2 i_y}{dt^2} - \frac{\ddot{\theta}}{\dot{\theta}^2} \frac{di_y}{dt}\right) - \frac{R}{K}\left(\frac{1}{\dot{\theta}} \frac{di_y}{dt} - \frac{\ddot{\theta}}{\dot{\theta}^2} i_y\right) \qquad (15)$$

substituting Eqs. (14) and (15) into (12) and grouping terms

$$-\frac{L^2}{K\dot\theta}\frac{d^2i_y}{dt^2}+\frac{L^2\ddot\theta}{K\dot\theta^2}\frac{di_y}{dt}-\frac{RL}{K\dot\theta}\frac{di_y}{dt}+\frac{RL\ddot\theta}{K\dot\theta^2}i_y-\frac{RL}{K\dot\theta}\frac{di_y}{dt}-\frac{R^2}{K\dot\theta}i_y+RN_mi_m=K\dot\theta i_y$$

$$\frac{L^2}{K\dot\theta}\frac{d^2i_y}{dt^2}+\left(\frac{2RL}{K\dot\theta}-\frac{L^2\ddot\theta}{K\dot\theta^2}\right)\frac{di_y}{dt}+\left(\frac{R^2}{K\dot\theta}+K\dot\theta-\frac{RL\ddot\theta}{K\dot\theta^2}\right)i_y=RN_mi_m$$

or

$$\frac{d^2i_y}{dt^2}+\left(\frac{2R}{L}-\frac{\ddot\theta}{\dot\theta}\right)\frac{di_y}{dt}+\left[\left(\frac{R}{L}\right)^2+\left(\frac{K\dot\theta}{L}\right)^2-\frac{R\ddot\theta}{L\dot\theta}\right]i_y=\left(\frac{RKN_mi_m}{L^2}\right)\dot\theta \quad (16)$$

This is the equation for the current symmetrical about the Y-axis. Since

$$\mathcal{F}_y=\frac{4\pi}{10}i_y \qquad \text{gilberts}$$

$$\phi_y=\frac{4\pi}{10\mathcal{R}}i_y$$

$$e_{out}=\frac{4\pi}{10^9}\frac{N_Y}{\mathcal{R}}\frac{di_y}{dt} \qquad \text{volts} \quad (17)$$

Theoretically, i_y is proportional to $\dot\theta$. Therefore the theoretical performance equation should be

$$\left(\frac{R}{L}\right)^2i_y=N_mi_m\frac{RK}{L^2}\dot\theta$$

or

$$i_y=N_mi_m\frac{K}{R}\dot\theta$$

and

$$\frac{di_y}{dt}=N_mi_m\frac{K}{R}\ddot\theta$$

then

$$e_{out}=\left(\frac{4\pi}{10^9}\right)\left(\frac{N_YN_mi_m}{\mathcal{R}}\right)\left(\frac{K}{R}\right)\ddot\theta=K_\alpha\ddot\theta \quad (18)$$

where K_α is the theoretical acceleration proportionality constant.

Solving Eq. (13) for $\frac{dy}{dt}$ and substituting this into Eq. (17), results in what is considered the actual performance equation.

The actual performance equation will be expressed as

$$e_{out} = K_{\alpha}[DF]\ddot{\theta} \tag{19}$$

where $[DF]$ is defined as the deviation function for the particular type of forcing function, $\ddot{\theta}$.

$$[DF] = \frac{\text{actual performance equation}}{\text{theroretical performance equation}}$$

Introduction

When Eq. (16) is examined it appears that the ratio $\ddot{\theta}/\dot{\theta}$ will tend to go to infinity at any time $\dot{\theta}$ approaches zero. Rearranging Eq. (16) as follows

$$\frac{d^2 i_y}{dt^2} + \frac{2R}{L}\frac{di_y}{dt} + \left[\left(\frac{R}{L}\right)^2 + \left(\frac{K\dot{\theta}}{L}\right)^2\right] i_y - \frac{\ddot{\theta}}{L\dot{\theta}}\left[L\frac{di_y}{dt} + R\, i_y\right] = N_m i_m \frac{RK}{L^2}\,\dot{\theta} \qquad (20)$$

By extracting the last term on the left side of Eq. (20) and replacing the term in brackets with the right hand term of Eq. (11), the following is obtained

$$\frac{\ddot{\theta}}{L\dot{\theta}}\left[K\dot{\theta}(N_m i_m - i_x)\right] = \frac{\ddot{\theta}}{L\dot{\theta}}\left[L\frac{di_y}{dt} + R i_y\right] \qquad (21)$$

Now it becomes apparent that as $\dot{\theta}$ approaches zero the term $\ddot{\theta}/\dot{\theta}$ is always finite.

Since the performance equation cannot be solved explicitly for i_y, it is necessary to solve the equation in general terms using various functions for $\dot{\theta}$ which will represent the practical use of the device.

The tachometer will normally be connected to a servo motor shaft or other shaft so that the output of the tachometer, used as an accelerometer, will be an indication of the shaft acceleration. Use in this manner suggests two types of shaft motion.

The first shaft motion considered will be sinusoidal.

This type motion is important due to the practice of designing servomechanisms based on desired or specified frequency response characteristics, which necessitates testing with a sinusoidal input.

The other type of shaft motion considered is that of a shaft coming up to speed as the result of a step voltage input to the control phase of a servo motor. This action results in the shaft coming up to steady state speed, approximately, exponentially. The solution for the exponential type motion also results in the steady state sensitivity of the accelerometer when used in a speed regulating system to indicate shaft accelerations about the regulated speed.

Performance Equation for Sinusoidal Motion

Sinusoidal motion is described by the following equations

$$\theta = \theta_m \cos \omega t + C$$
$$\dot{\theta} = -\theta_m \omega \sin \omega t$$
$$\ddot{\theta} = -\theta_m \omega^2 \cos \omega t$$

where θ_m* is the maximum angular shaft displacement from its center position and ω is the angular velocity of the forcing mechanism.

Considering Eq. (12) and assuming that

$$\frac{L}{R}\frac{di_x}{dt} \ll i_x$$

then

$$i_x \approx \frac{K\dot{\theta}}{R} i_y \qquad (22)$$

*See Fig. 4-7

Now substituting this expression for i_x into Eq. (21) and then substituting the resulting equation into Eq. (20), the following is obtained.

$$\frac{d^2 i_y}{dt^2} + \frac{2R}{L}\frac{di_y}{dt} + \left[\left(\frac{R}{L}\right)^2 + \left(\frac{K\dot{\theta}}{L}\right)^2 + \frac{K^2\dot{\theta}\ddot{\theta}}{RL}\right] i_y = N_m i_m \frac{K}{L}\left[\ddot{\theta} + \frac{R}{L}\dot{\theta}\right] \qquad (23)$$

Now if it is assumed* that

$$\left(\frac{R}{L}\right)^2 \gg \left(\frac{K\dot{\theta}}{L}\right)^2 + \frac{K^2\dot{\theta}\ddot{\theta}}{RL}$$

then Eq. (23) becomes

$$\frac{di_y}{dt} + \frac{R}{L} i_y = N_m i_m \frac{K}{L}\dot{\theta} \qquad (24)$$

A comparison between Eqs. (24) and (11) shows that i_x has been implicitly assumed small compared to $N_m i_m$.

When Eqs. (24) and (17) are solved in Laplace Transform notation (using s as the Laplacian operator) the following equation is obtained

$$e_{out}(s) = \frac{K\alpha\,\ddot{\theta}(s)}{\tau s + 1} \qquad (25)$$

where τ equals L/R. When Eq. (25) is solved as a function of time, and using $\ddot{\theta} = -\theta_m \omega^2 \cos\omega t$, the following equation is obtained.

$$e = -\frac{K\alpha\theta_m\omega^2}{\left[\left(\frac{L\omega}{R}\right)^2+1\right]^{1/2}}\left\{\frac{-e^{-\frac{R}{L}t}}{\left[\left(\frac{L\omega}{R}\right)^2+1\right]^{1/2}} + \cos(\omega t - \psi)\right\}$$

where

$$\psi = \tan^{-1}\frac{L\omega}{R}$$

After the transient has passed, the steady state output

*Refer to Table 3-2 for the validation of this assumption.

Table 3-1. Constants for ARMA 1B400 INDUCTION GENERATOR

ℓ = 2.163 cm	R = 2.95×10^{-4} ohms
ℓ = 0.0982 cm	L = 2.80×10^{-7} henrys
ρ = 14.9 μohm-cm	K = 5.35×10^{-7} cm
r = 1.9340 cm	
t = 0.0380 cm	K/L = 1050
$\mathcal{R}$ = 0.0149 cm^{-1}	K/R = 1.81×10^{-3}

Table 3-2. Comparison of terms in the dependent variable coefficient.

Values of constants from Table 3-1
$\dot{\theta} = (1/8)100\pi\cos 100\pi t$

ωt degrees	$(R/L)^2 \times 10^{-6}$	$\left[(K\dot{\theta}/L)^2 + (K^2\dot{\theta}\ddot{\theta}/RL)\right] \times 10^{-3}$
0	1.11	0.00
10	1.11	0.34
20	1.11	1.19
30	1.11	2.13
40	1.11	3.15
50	1.11	4.12
60	1.11	4.94
70	1.11	5.49
80	1.11	5.62
90	1.11	5.62
100	1.11	5.28
110	1.11	4.41
120	1.11	3.48
130	1.11	2.47
140	1.11	1.50
150	1.11	0.67
160	1.11	0.80
170	1.11	0.00
180	1.11	0.00

voltage expression becomes

$$e_{out} = K_\alpha [DF]_s \ddot{\theta} \tag{26}$$

where $[DF]_s$ is the Sinusoidal Deviation Function.

$$[DF]_s \triangleq \frac{e^{-j\psi}}{\left[\left(\frac{L\omega}{R}\right)^2 + 1\right]^{1/2}} \tag{27}$$

Since this solution is based on the assumption that $i_x \ll N_m i_m$, the value of i_x will be found.

From the steady state solution of Eq. (24)

$$i_y = -N_m i_m \frac{K}{R} \theta_m \omega \frac{\sin(\omega t - \psi)}{\left[\left(\frac{L\omega}{R}\right)^2 + 1\right]^{1/2}} \tag{28}$$

but from Eq. (10)

$$\frac{di_x}{dt} + \frac{R}{L} i_x = \frac{K\dot{\theta}}{L} i_y \tag{29}$$

By solving Eqs. (28) and (29) for i_x, it can be shown that

$$i_x < \left[\frac{K\theta_m\omega}{R}\right] N_m i_m$$

$$i_x < 5.6 \times 10^{-3} N_m i_m$$

This verifies the assumption and therefore Eqs. (24), (26), and (27), are valid for an AN A 18400 INDUCTION GENERATOR if $\omega \leq 100\pi$.

Performance Equation for Exponential Motion

Exponential motion is described by the following

equations:

$$\dot{\theta} = S_o\left(1 - e^{-t/\tau}\right) \qquad = S_o\left(1 - e^{-z}\right)$$

$$\ddot{\theta} = S_o/\tau\, e^{-t/\tau} \qquad = S_o/\tau\, e^{-z}$$

where S_o is the steady state speed in radians per second, τ is the time constant of the exponential curve and $z = t/\tau$ is a new independent variable.

Figs. 4-3 (a) and 4-3 (b) show the comparison of the assumption of exponential shaft motion and that actually obtained by applying a voltage step to the control phase of a two-phase servomotor.

Since in the exponential motion application, the cup has to come up to speed from zero. $\dot{\theta}$ and i_x both start at zero and $\left(\frac{K\dot{\theta}}{L}\right)^2$ remains low, compared to $(R/L)^2$, until $\dot{\theta}$ becomes of significant magnitude. Also i_x starts out at zero and remains low, compared to $N_m i_m$, near zero. Using these two assumptions, and Eq. (21), Eq.(20) now becomes

$$\frac{d^2 i_y}{dt^2} + \left(\frac{2R}{L}\right)\frac{di_y}{dt} + \left(\frac{R}{L}\right)^2 i_y = N_m i_m \frac{K}{L}\left(\frac{d\dot{\theta}}{dt} + \frac{R}{L}\dot{\theta}\right) \qquad (30)$$

or by simplification

$$\frac{di_y}{dt} + \frac{R}{L} i_y = N_m i_m \frac{K}{L}\dot{\theta}$$

which is the same as Eq. (24).

Making the exponential substitution for $\dot{\theta}$ and changing the variable

$$\frac{di_{y(z)}}{dz} + \frac{\tau R}{L} i_{y(z)} = N_m i_m \frac{\tau K S_o}{L}\left(1 - e^{-z}\right)$$

solving this equation for $i_y(z)$ by Laplace Transformations

$$i_y(t) = N_m i_m \frac{K}{R} S_o \left[1 - \frac{\frac{\tau R}{L} e^{-t/\tau} - e^{-\frac{R}{L}t}}{\frac{\tau R}{L} - 1} \right] \qquad (31)$$

$$\frac{di_y(t)}{dt} = N_m i_m \frac{K}{R} S_o \left[\frac{\frac{R}{L} e^{-t/\tau} - \frac{R}{L} e^{-\frac{R}{L}t}}{\frac{\tau R}{L} - 1} \right]$$

or factoring out $S_o/\tau e^{-t/\tau}$, which is $\ddot{\theta}$ and K/I

$$\frac{di_y}{dt} = N_m i_m \frac{K}{R} \left[\frac{1 - e^{\left(\frac{1}{\tau} - \frac{R}{L}\right)t}}{1 - \frac{L}{\tau R}} \right] \ddot{\theta}$$

or since $R/I \gg 1$

$$\frac{di_y}{dt} = N_m i_m \frac{K}{R} \left[1 - e^{-\frac{R}{L}t} \right] \ddot{\theta} \qquad (32)$$

Due to the limitation placed on this solution, it is necessary to determine when the term i_x becomes significant when compared to $N_m i_m$.

The expression for i_x is obtained from Eq. 14

$$i_x(t) = N_m i_m - \frac{L}{K\dot{\theta}} \frac{di_y(t)}{dt} - \frac{R}{K\dot{\theta}} i_y(t) \qquad (33)$$

but when substituting Eqs. (31) and (32) and the expression for $\dot{\theta}$ into Eq. (33), the value of $i_x(t)$ is always zero.

This indicates that $i_x(t)$ remains at zero until the form of the equation changes. This will happen when the value of $\left(\frac{K\dot{\theta}}{L}\right)^2$ becomes of a significant value when compared to $(R/L)^2$.

Using the values for the motor 1540 as shown in Table 3-1 and $\dot{\theta} = 514 \left(1 - e^{-t/0.286}\right)$.

$$\frac{\left(\frac{R}{L}\right)^2}{\left(\frac{K\dot{\theta}}{L}\right)^2} = 340 \qquad \text{for} \quad t = 0.03 \text{ seconds}$$

$\frac{K\dot{\theta}}{L}$ increases in value with t and is considered after t = 0.03. At t = 0.03, the quantity $\ddot{\theta}/\dot{\theta}$ has a value of 3.37 and is decreasing rapidly, so that it can now be neglected.

Therefore after t = 0.03 the equation becomes

$$\frac{d^2 i_y(t)}{dt^2} + \left(\frac{2R}{L}\right)\frac{d i_y(t)}{dt} + \left[\left(\frac{R}{L}\right)^2 + \left(\frac{K\dot{\theta}}{L}\right)^2\right] i_y(t) = \frac{N_m i_m RK}{L^2}\dot{\theta} \qquad (54)$$

Since the value of $\left[\left(\frac{R}{L}\right)^2 + \left(\frac{K\dot{\theta}}{L}\right)^2\right]$ changes slowly with t, it is considered as a constant during the remainder of the solution. Table 3-3 shows the variation of the term $\left[\left(\frac{R}{L}\right)^2 + \left(\frac{K\dot{\theta}}{L}\right)^2\right]$ with t.

Table 3-3. Value of dependent variable coefficient

time	$\left(\frac{K}{L}\dot{\theta}\right)^2 \times 10^5$	$\left[\left(\frac{R}{L}\right)^2 + \left(\frac{K}{L}\dot{\theta}\right)^2\right] \times 10^5$
0.03	0.035	11.00
0.06	0.105	10.85
0.09	0.241	10.79
0.15	0.592	10.64
0.30	1.420	9.61
0.60	2.330	8.70
0.90	3.250	7.78
1.20	3.470	7.58
1.50	3.540	7.49
1.80	3.580	7.45
2.10	3.596	7.43
2.40	3.600	7.43

Changing variables and substituting for $\dot{\theta}$

$$\frac{d^2 i_y(z)}{dz^2} + \left(\frac{2TR}{L}\right)\frac{d i_y(z)}{dz} + \left[\left(\frac{TR}{L}\right)^2 + \left(\frac{TK\dot{\theta}}{L}\right)^2\right] i_y(z) = N_m i_m \frac{RK T^2 S_o}{L^2}\left(1 - e^{-z}\right)$$

solving this equation for $i_y(z)$ by Laplace Transforms and

changing the variable back to t/τ

$$i_y(t) = \frac{N_m i_m R K \tau^2 S_o}{L^2}\left[\frac{1}{\left(\frac{\tau R}{L}\right)^2+\left(\frac{\tau K\dot\theta}{L}\right)^2} - \frac{e^{-t/\tau}}{\left(\frac{\tau R}{L}-1\right)^2+\left(\frac{\tau K\dot\theta}{L}\right)^2}\right.$$

$$\left. + \frac{e^{-\frac{R}{L}t}\sin\left(\frac{K\dot\theta}{L}t-\psi\right)}{\frac{\tau K\dot\theta}{L}\left[\left(\frac{\tau R}{L}\right)^2+\left(\frac{\tau K\dot\theta}{L}\right)^2\right]^{1/2}\left[\left(1-\frac{\tau R}{L}\right)^2+\left(\frac{\tau K\dot\theta}{L}\right)^2\right]^{1/2}}\right]$$

$$\psi \triangleq \tan^{-1}\frac{K\dot\theta}{-R} + \tan^{-1}\frac{K\dot\theta}{\left(\frac{L}{\tau R}-1\right)R}$$

Since this equation is only for values of $t > 0.05$ and since $R/L \approx 1000$, the last term can be neglected. Also $\tau R/L >> 1$ so the resulting equation becomes

$$i_y(t) = N_m i_m \frac{RK\tau^2 S_o}{L^2}\,\frac{1-e^{-t/\tau}}{\left(\frac{\tau R}{L}\right)^2+\left(\frac{\tau K\dot\theta}{L}\right)^2}$$

or

$$i_y(t) = N_m i_m \frac{K}{R}\left[\frac{1}{1+\left(\frac{K\dot\theta}{R}\right)^2}\right]\dot\theta \qquad (55)$$

$$\frac{di_y(t)}{dt} = N_m i_m \frac{K}{R}\,\frac{\left[1+\left(\frac{K\dot\theta}{R}\right)^2\right]\ddot\theta - \dot\theta 2\left(\frac{K}{R}\right)^2\dot\theta\ddot\theta}{\left[1+\left(\frac{K\dot\theta}{R}\right)^2\right]^2}$$

$$= N_m i_m \frac{K}{R}\left\{\frac{1-\left(\frac{K\dot\theta}{R}\right)^2}{\left[1+\left(\frac{K\dot\theta}{R}\right)^2\right]^2}\right\}\ddot\theta \qquad (56)$$

Now since

$$e_{out} = \frac{4\pi N_r}{10^9 R}\frac{di_y}{dt} = \frac{4\pi N_r N_m i_m}{10^9 R}\frac{K}{R}\left[DF\right]\ddot\theta$$

$$= K_\alpha\left[DF\right]\ddot\theta$$

where, considering Eqs. (33) and (35)

$$[DF]_{E1} = 1 - e^{-\frac{R}{L}t} \qquad \text{from } t = 0 \text{ to } t = 0.03$$

$$[DF]_{E2} = \frac{1 - \left(\frac{K\dot{\theta}}{R}\right)^2}{\left[1 + \left(\frac{K\dot{\theta}}{R}\right)^2\right]^2} \qquad \text{from } t = 0.03 \text{ to infinity}$$

Computer Comparison for the Derived Performance Equations

The Math Department of the M.I.T. Instrumentation Laboratory, programmed the IBM 650 computer for the simultaneous solution of Eqs. (11) and (12) using the values of the constants for the [illegible] 1B400 INDUCTION GENERATOR as listed in Table 3-1 and the following forcing functions:

$$\dot{\theta} = 314\left(1 - e^{-t/0.286}\right)$$

and

$$\dot{\theta} = \theta_m \omega \sin \omega t$$

where

$$\theta_m = 1/8 \text{ radian}$$
$$\omega = 100\pi \text{ radians/second}$$

The results of the computer solution served as a means of checking the assumptions made in the derivations for the Actual Performance Equations. The results of some of the computer comparisons are shown on Figs. 3-1, 3-2, 3-3, and 3-4.

For both types of motion the IBM 650 provided, as part of its solution, the ratio $\left(\dot{I}_y / N_m i_m \frac{K}{R}\right)$ which represents what has been defined as the Deviation Function.

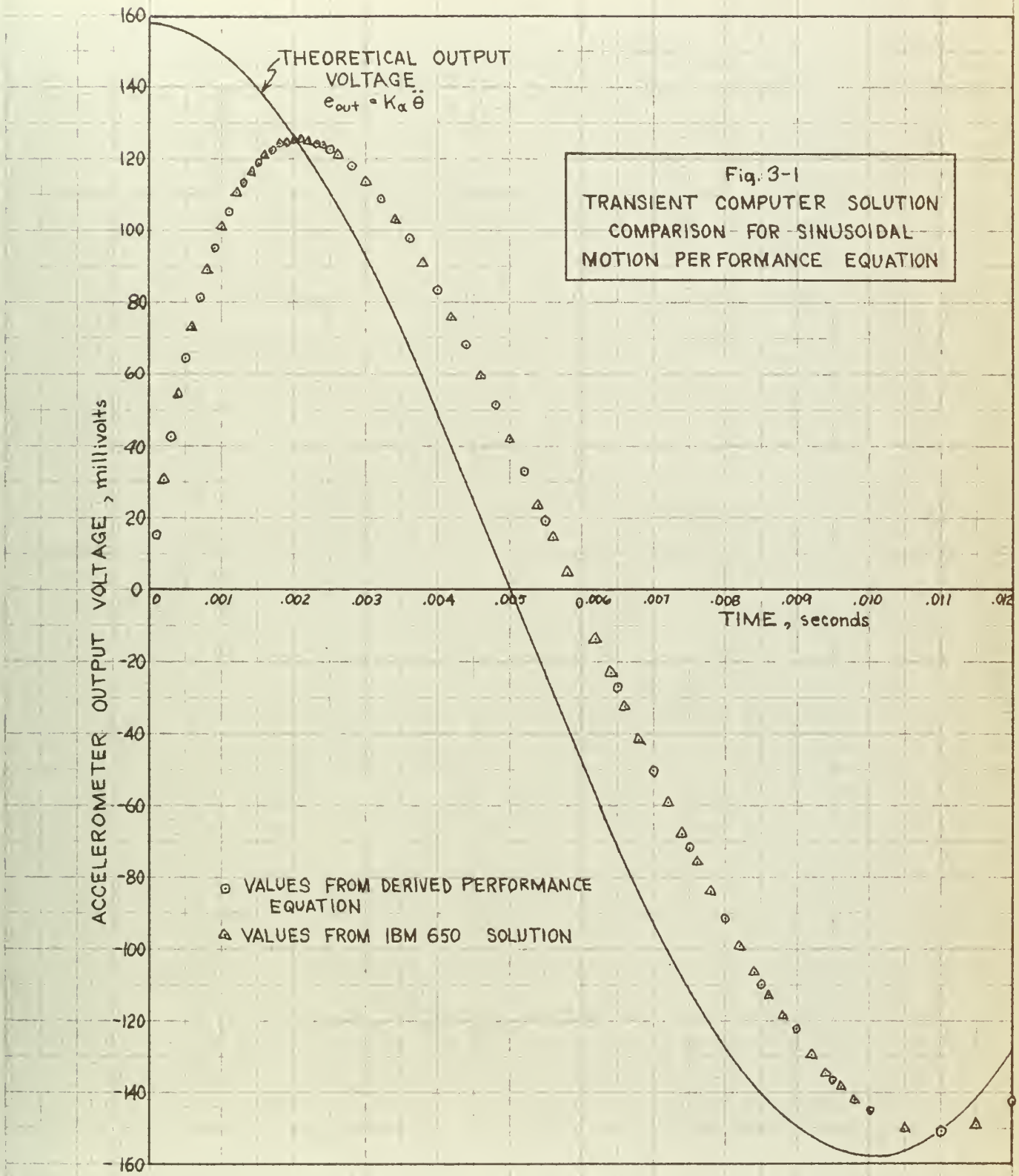

Fig. 3-1
TRANSIENT COMPUTER SOLUTION COMPARISON FOR SINUSOIDAL MOTION PERFORMANCE EQUATION

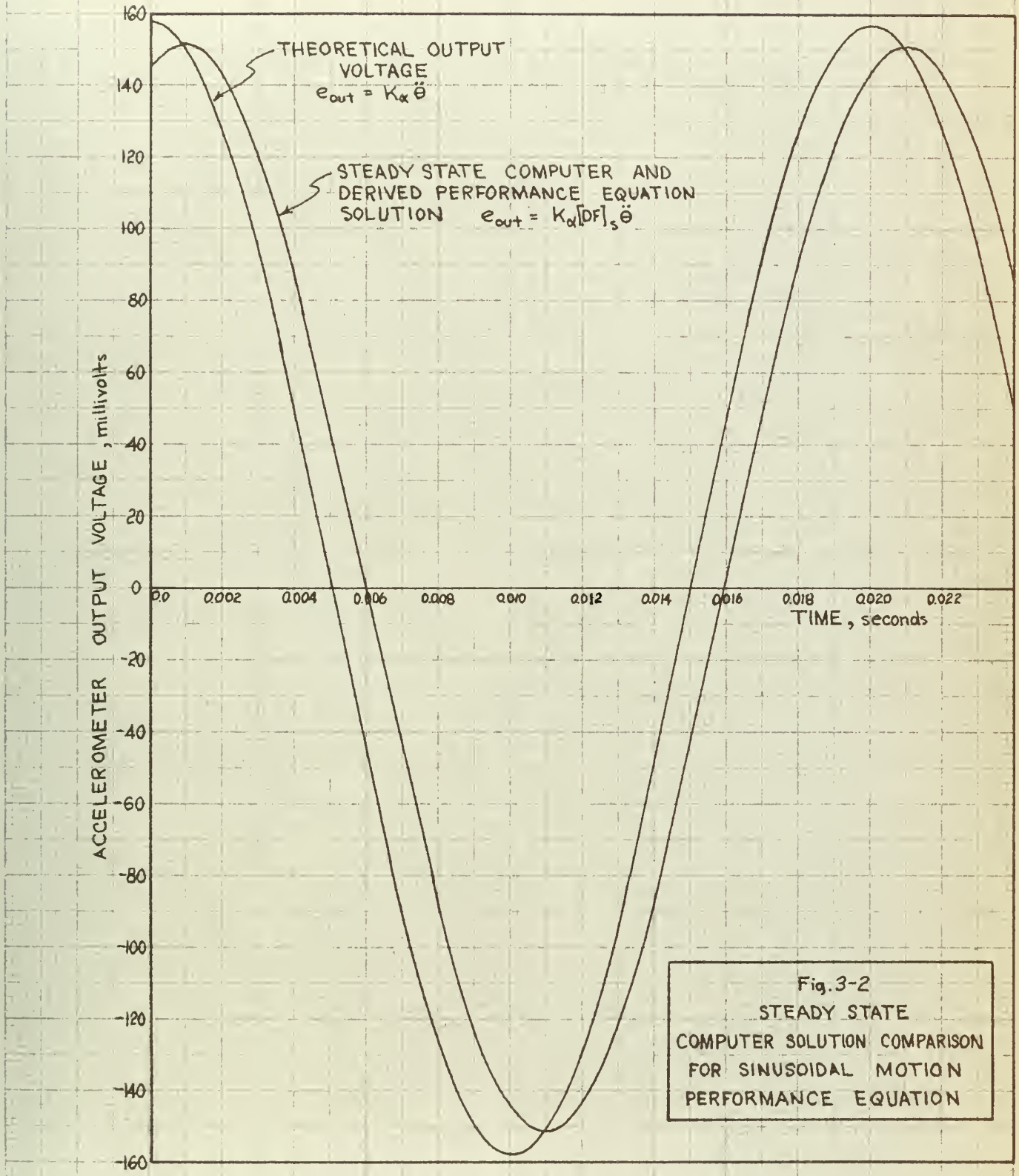

Fig. 3-2
STEADY STATE
COMPUTER SOLUTION COMPARISON
FOR SINUSOIDAL MOTION
PERFORMANCE EQUATION

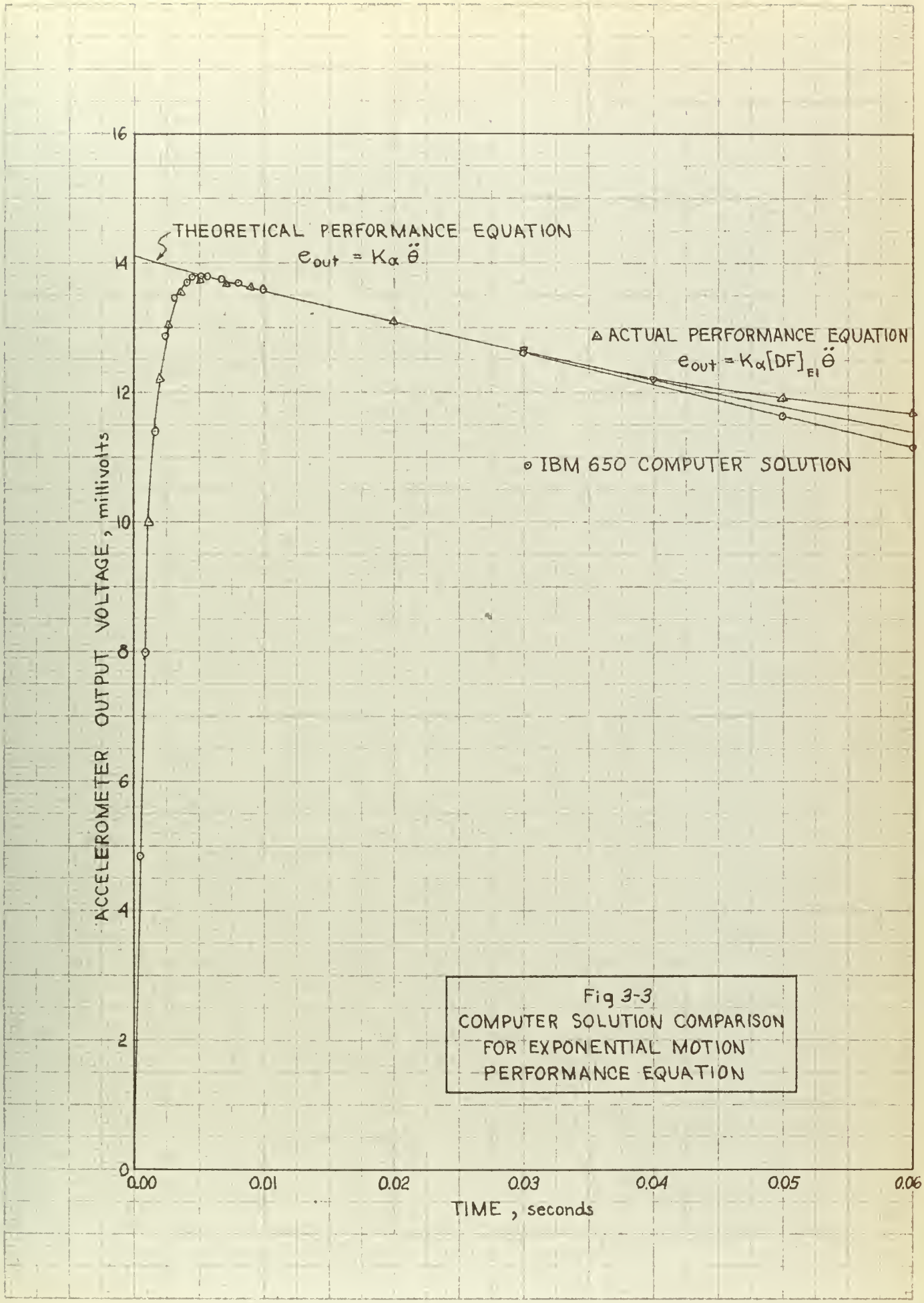

Fig 3-3
COMPUTER SOLUTION COMPARISON
FOR EXPONENTIAL MOTION
PERFORMANCE EQUATION

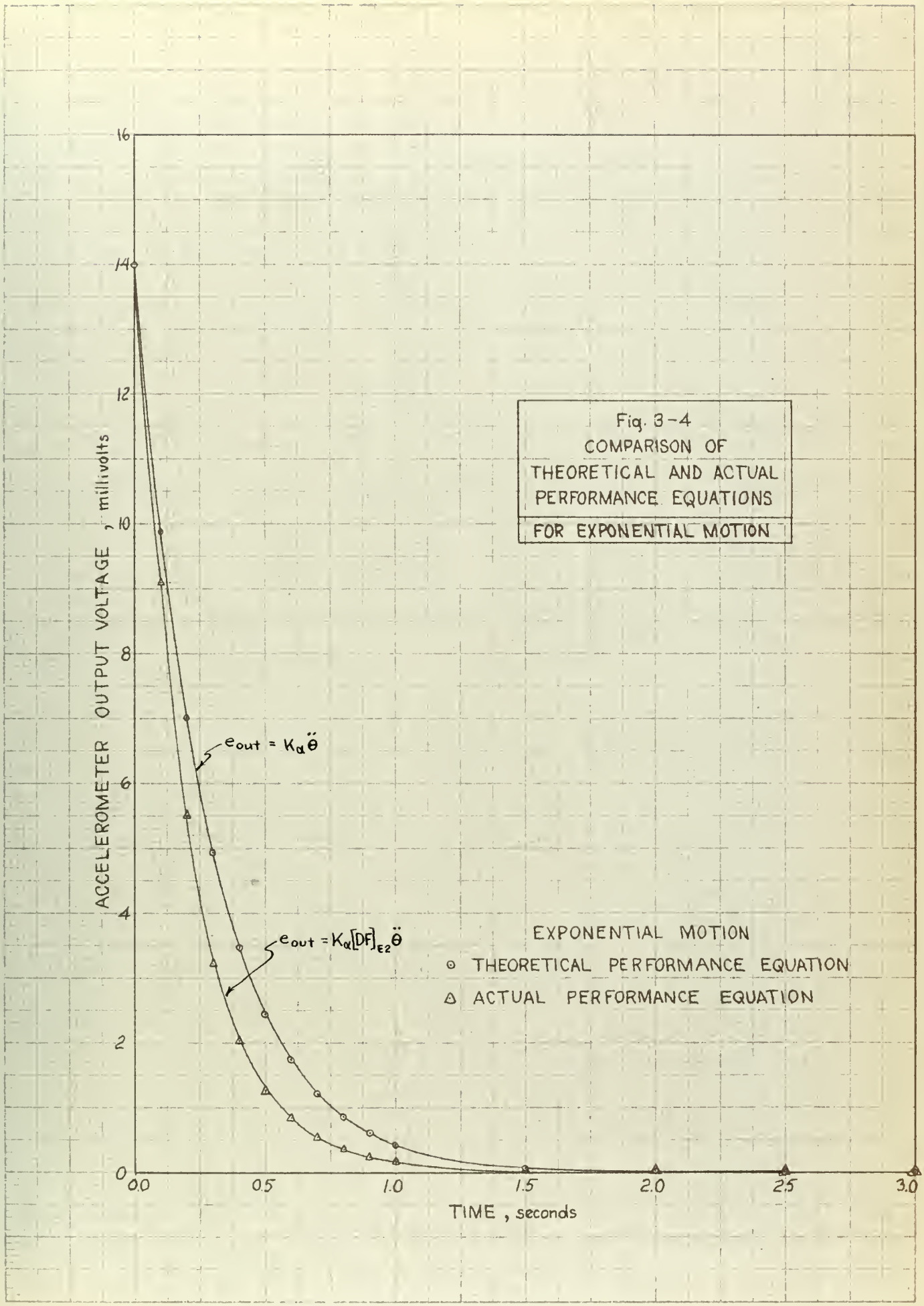

Fig. 3-4
COMPARISON OF
THEORETICAL AND ACTUAL
PERFORMANCE EQUATIONS
FOR EXPONENTIAL MOTION

For sinusoidal motion, where the derived Deviation Function is

$$[DF]_s = \frac{e^{-j\psi}}{\left[1 + \left(\frac{\omega L}{R}\right)^2\right]^{1/2}}$$

the following comparison resulted:

$$\text{IBM 650} \qquad [DF] = \frac{1}{1.046} e^{-j\,0.282}$$

$$\text{Derived value} \qquad [DF]_s = \frac{1}{1.044} e^{-j\,0.290}$$

In the derivation for the Sinusoidal Deviation Function, the value of i_x was assumed to be small compared to $N_m i_m$. A check on this assumption was made by having the IBM 650 compute the value for i_x. The maximum value of i_x from the computer solution was 0.09 while $N_m i_m$ is 20.65. This comparison verifies the assumption used to obtain the Sinusoidal Deviation Function.

For exponential motion, the IBM 650 Computer was used to solve the equations up to t = 0.03 seconds, where the Exponential Deviation Function changed form.

Table 3-4 gives a comparison between the IBM 650's values for $\left(\dot{I}_y / N_m i_m \frac{K}{R}\right)$ and those obtained from the derived Exponential Deviation Function, which is

$$[DF]_{E1} = 1 - e^{-\frac{R}{L}t}$$

The derivation for the Exponential Deviation Function, $[DF]_{E1}$, also assumes that, for time prior to 0.03 seconds, the value of i_x is small compared to $N_m i_m$. The IBM 650 Computer solved for i_x and at t = 0.03 seconds, i_x = 0.0605

Table 3-4. Values obtained for Exponential Deviation Function

Time	From IBM 650	From $[DF]_{E1}$
0.0004	0.3444	0.3430
0.0012	0.7186	0.7163
0.0020	0.8803	0.8775
0.0040	0.9880	0.9850
0.0060	1.0010	0.9982
0.0080	1.0030	0.9998
0.0090	1.0030	0.9999
0.0100	1.0030	1.0000
0.0200	1.0010	1.0000
0.0300	0.9972	1.0000

while $N_m i_m$ is 20.65. This comparison verifies the assumption used to obtain the Exponential Deviation Function for time prior to t = 0.03 seconds, and after this time the effect of the increasing i_x is included in the second Exponential Deviation Function which is

$$[DF]_{E2} = \frac{1 - \left(\frac{K\dot{\theta}}{R}\right)^2}{\left[1 + \left(\frac{K\dot{\theta}}{R}\right)^2\right]^2}$$

CHAPTER 4

TESTS CONDUCTED

Introduction

In order to confirm the effectiveness of an a-c tachometer used as an accelerometer, tests were conducted on the AMA 1B400, drag-cup type, induction generator. As has been previously stated, this choice was one of convenience. The tachometer (induction generator) used was connected on a common shaft with a modified BENDIX CK 3004, two-phase, 400 cps, induction motor. Figs. 4-1 and 4-2 show sketches of the test setup for the exponential motion and Table 4-1 describes the tachometer and motors used. For reasons that will be stated later, it was necessary to connect another motor (two-phase, 60 cps, induction motor) to the shaft extension of the 400 cps motor.

One of the usual test signals to servomechanisms is sinusoidal. Therefore it was desirable to test the accelerometer with sinusoidal motion. Another reason for this type of test was to provide two independent methods of checking the constants analytically derived. Also this type of test was used by Fowle [5] and Lovett [4] to obtain K_α, the acceleration proportionality constant, and it was part of the object of this thesis to verify or make limitations on their conclusions.

For the sinusoidal motion, the 60 cps motor was removed and the 400 cps motor shaft was connected directly to the sinusoidal stroking attachment of the M.I.T. Servomechanisms Laboratory Nine-Drive [10].

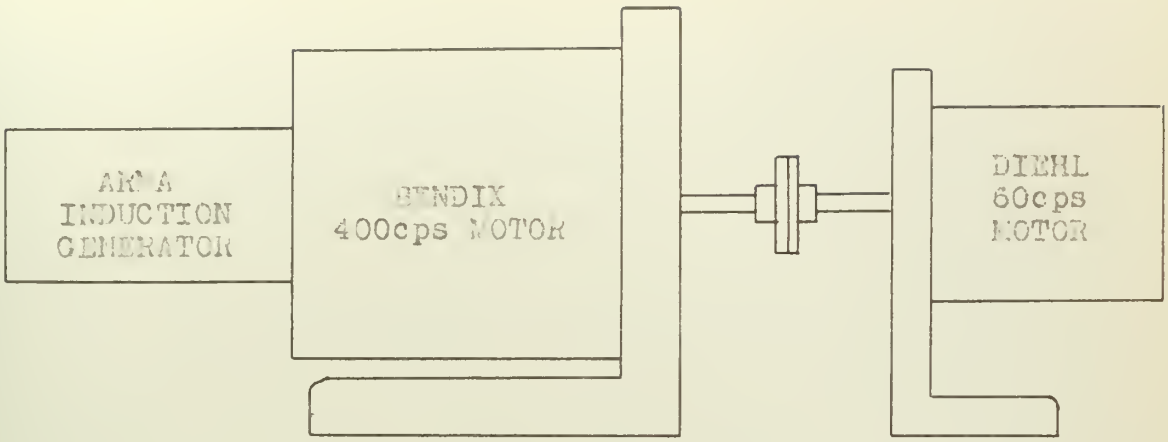

Fig. 4-1. Sketch of test set-up for exponential motion.

Table 4-1. Description of Units

ARMA 1B400 INDUCTION GENERATOR

4-pole, drag-cup type

Normal excitation 115 volts 400cps

BENDIX CK 3004 INDUCTION MOTOR

2-phase, 12-pole

Main field excitation 110 volts 400cps

Control Field excitation 220 volts 400cps

DIEHL CDA-211052 INDUCTION MOTOR

2-phase, 2-poles, 2/5 watts

Normal excitation 75/115 volts 60 cps

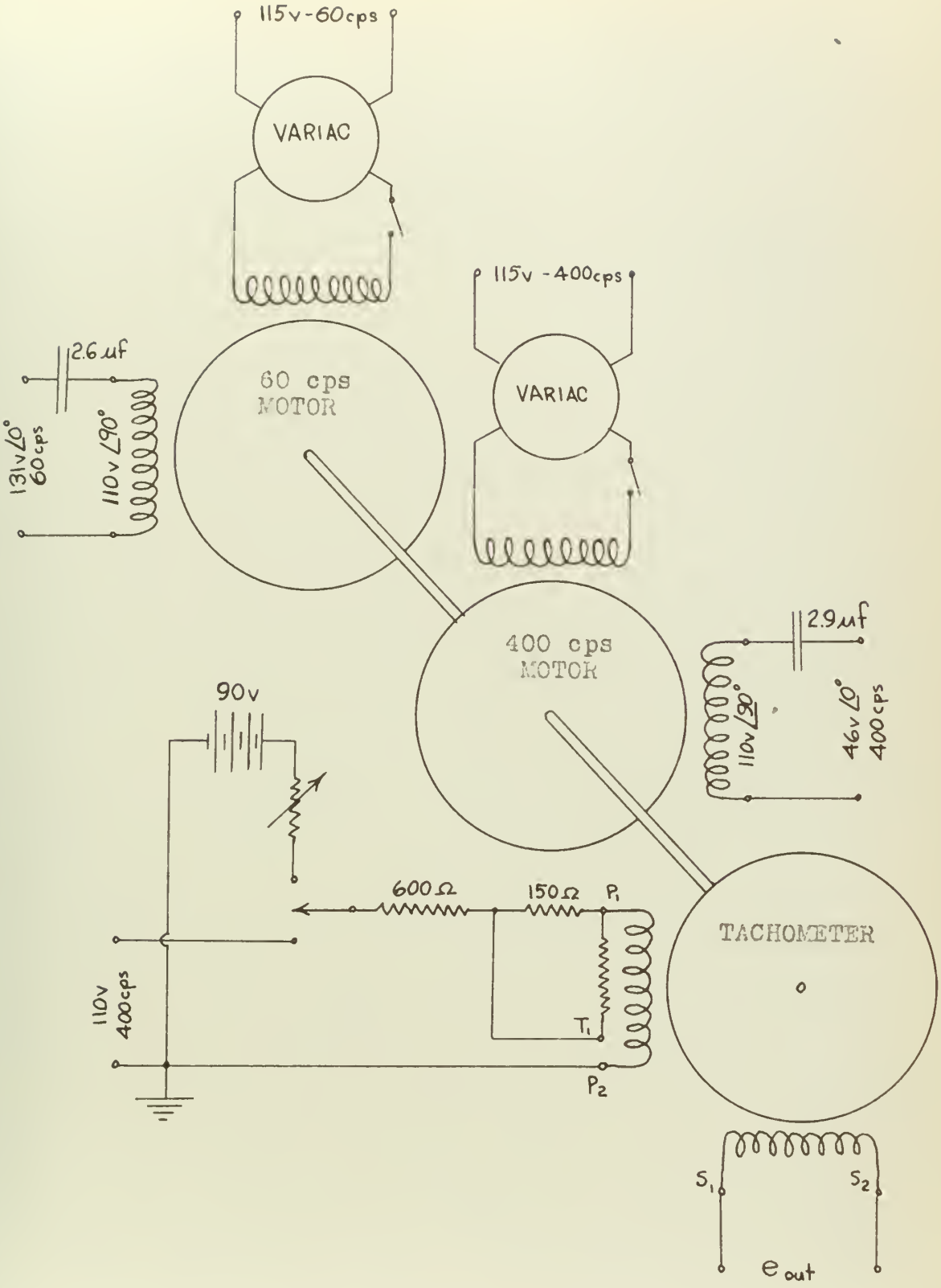

Fig. 4-2. Wiring diagram

Exponential Motion Tests

The purpose of this test was to provide the shaft of the tachometer with exponential motion that could be described by the equation

$$\dot{\theta}_{(t)} = S_o\left(1 - e^{-t/\tau}\right)$$

where S_o is the steady state speed and τ is the time constant of the exponential curve. It was felt that this could be done by applying a step voltage to the control phase winding of a two-phase induction motor. Figs. 4-3 (a) and 4-6 (a) show the shaft speed-time relationship resulting from this type of step input.

The first part of this test was to calibrate the control phase voltage setting to resulting shaft steady state speed. This calibration was done with a stroboscope. The tachometer was excited with 110 volts-400 cps and the output voltage read with various settings of the motor control phase voltage. The results of these calibrations are shown on Figs. 4-4 and 4-5.

With the tachometer calibrated, it was possible to determine the shaft steady state speed from the tachometer output voltage (when excited with 110v-400 cps).

The acceleration was measured by recording the tachometer output, when the tachometer was excited with d-c, on a Hanborn Recorder. The paper speed was approximately 100 mm/second. The actual time measurements were made by the use of a 60cps timing trace on the recorder tape.

For any particular set of readings, the steady state

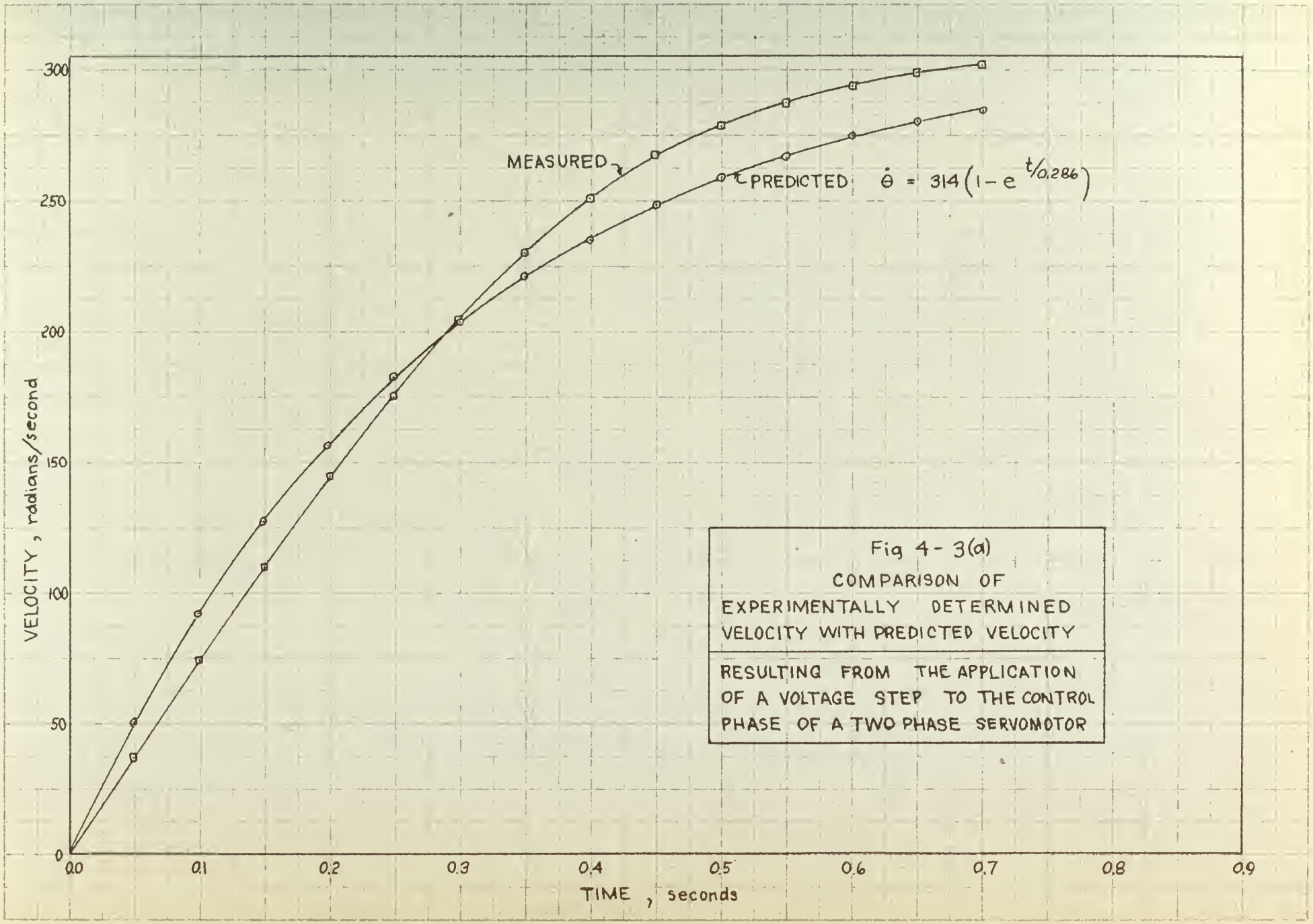

Fig 4-3(a)
COMPARISON OF EXPERIMENTALLY DETERMINED VELOCITY WITH PREDICTED VELOCITY RESULTING FROM THE APPLICATION OF A VOLTAGE STEP TO THE CONTROL PHASE OF A TWO PHASE SERVOMOTOR

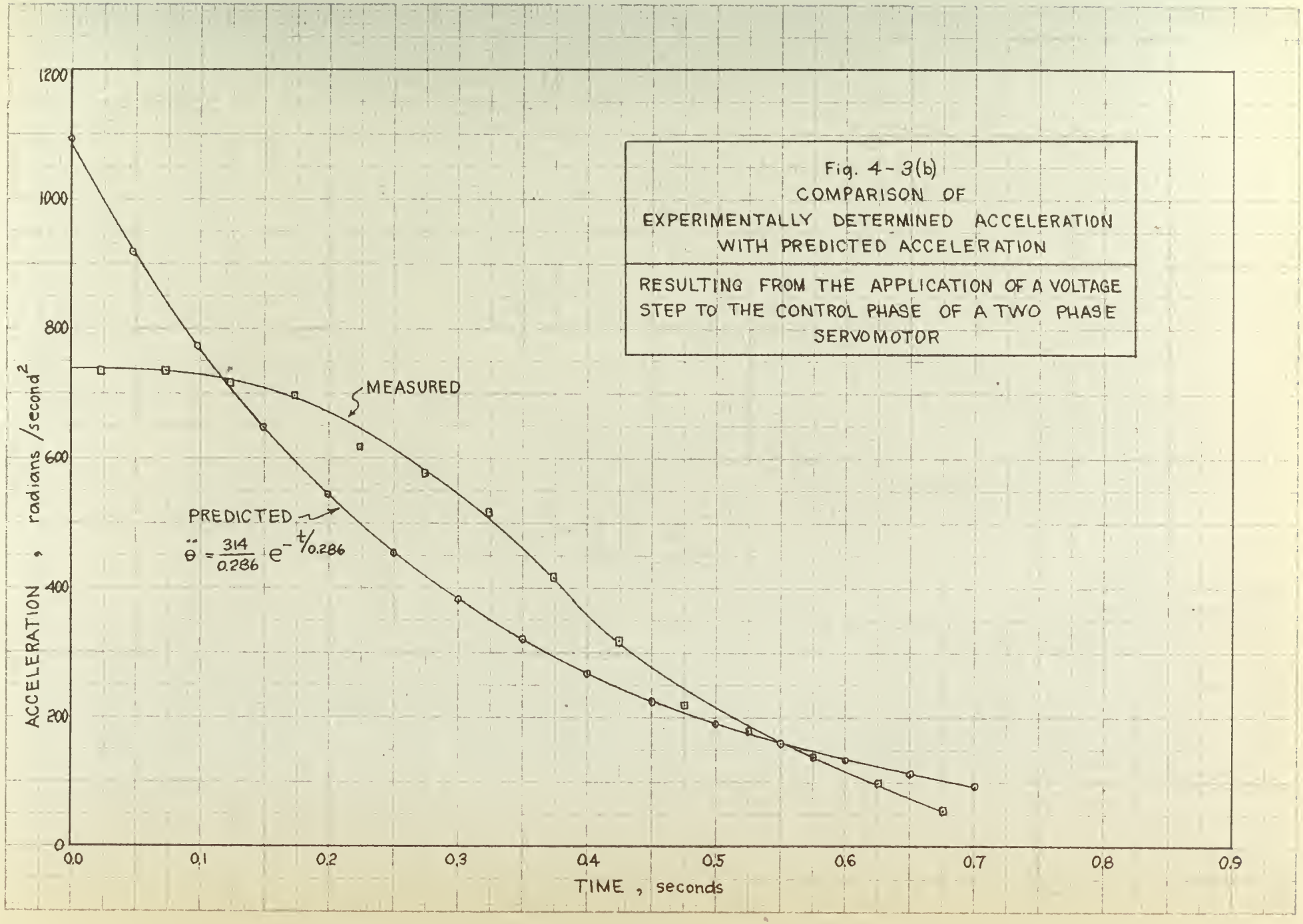
Fig. 4-3(b)
COMPARISON OF
EXPERIMENTALLY DETERMINED ACCELERATION
WITH PREDICTED ACCELERATION
RESULTING FROM THE APPLICATION OF A VOLTAGE STEP TO THE CONTROL PHASE OF A TWO PHASE SERVOMOTOR
MEASURED
PREDICTED
$\ddot{\theta} = \frac{314}{0.286} e^{-t/0.286}$
ACCELERATION , radians /second^2
TIME , seconds
0
200
400
600
800
1000
1200
0.0
0.1
0.2
0.3
0.4
0.5
0.6
0.7
0.8
0.9

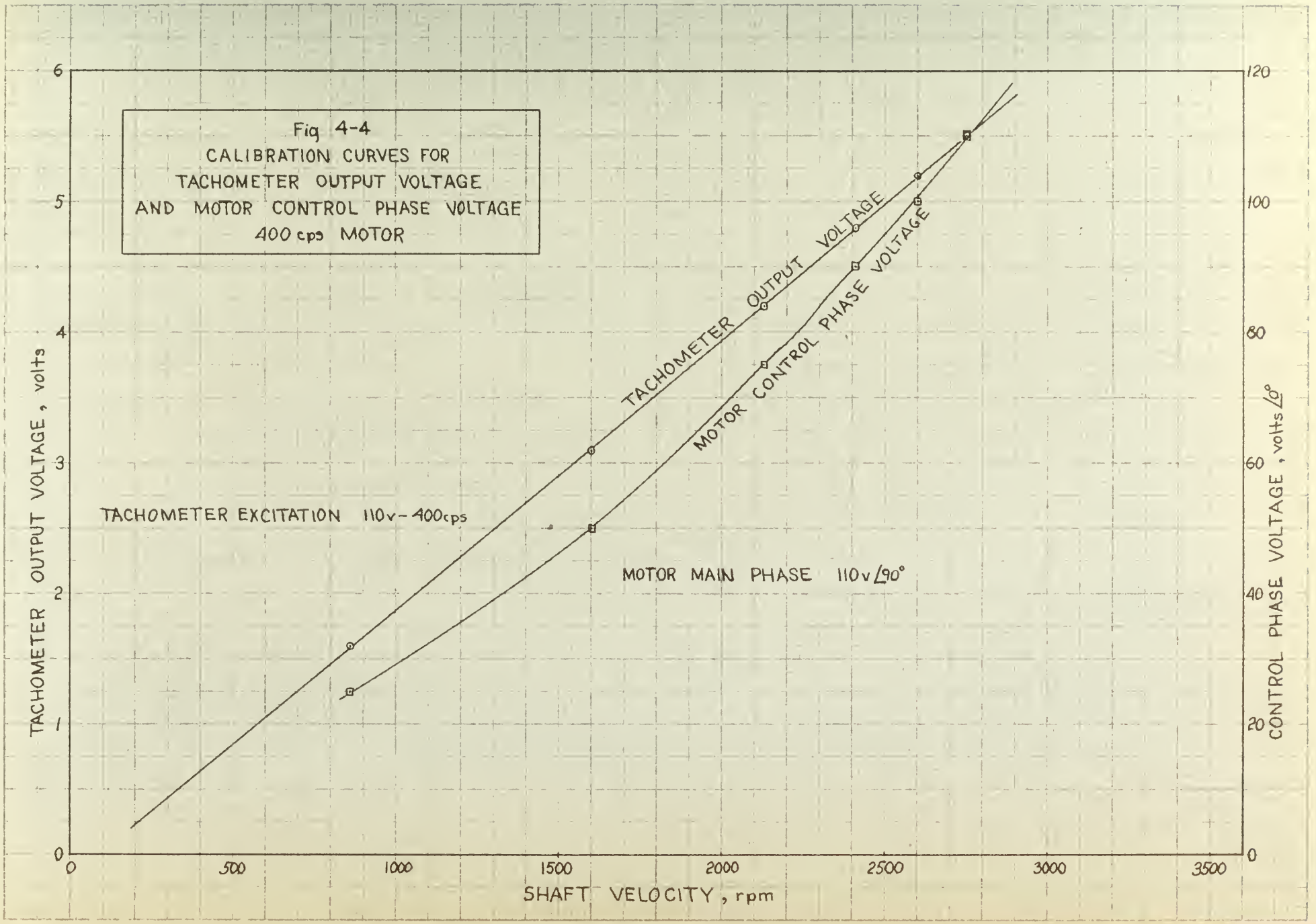
Fig 4-4
CALIBRATION CURVES FOR
TACHOMETER OUTPUT VOLTAGE
AND MOTOR CONTROL PHASE VOLTAGE
400 cps MOTOR
TACHOMETER OUTPUT VOLTAGE
MOTOR CONTROL PHASE VOLTAGE
TACHOMETER EXCITATION 110v - 400cps
MOTOR MAIN PHASE 110v ∠90°
TACHOMETER OUTPUT VOLTAGE, volts
CONTROL PHASE VOLTAGE, volts ∠0°
SHAFT VELOCITY, rpm
0
1
2
3
4
5
6
20
40
60
80
100
120
500
1000
1500
2000
2500
3000
3500

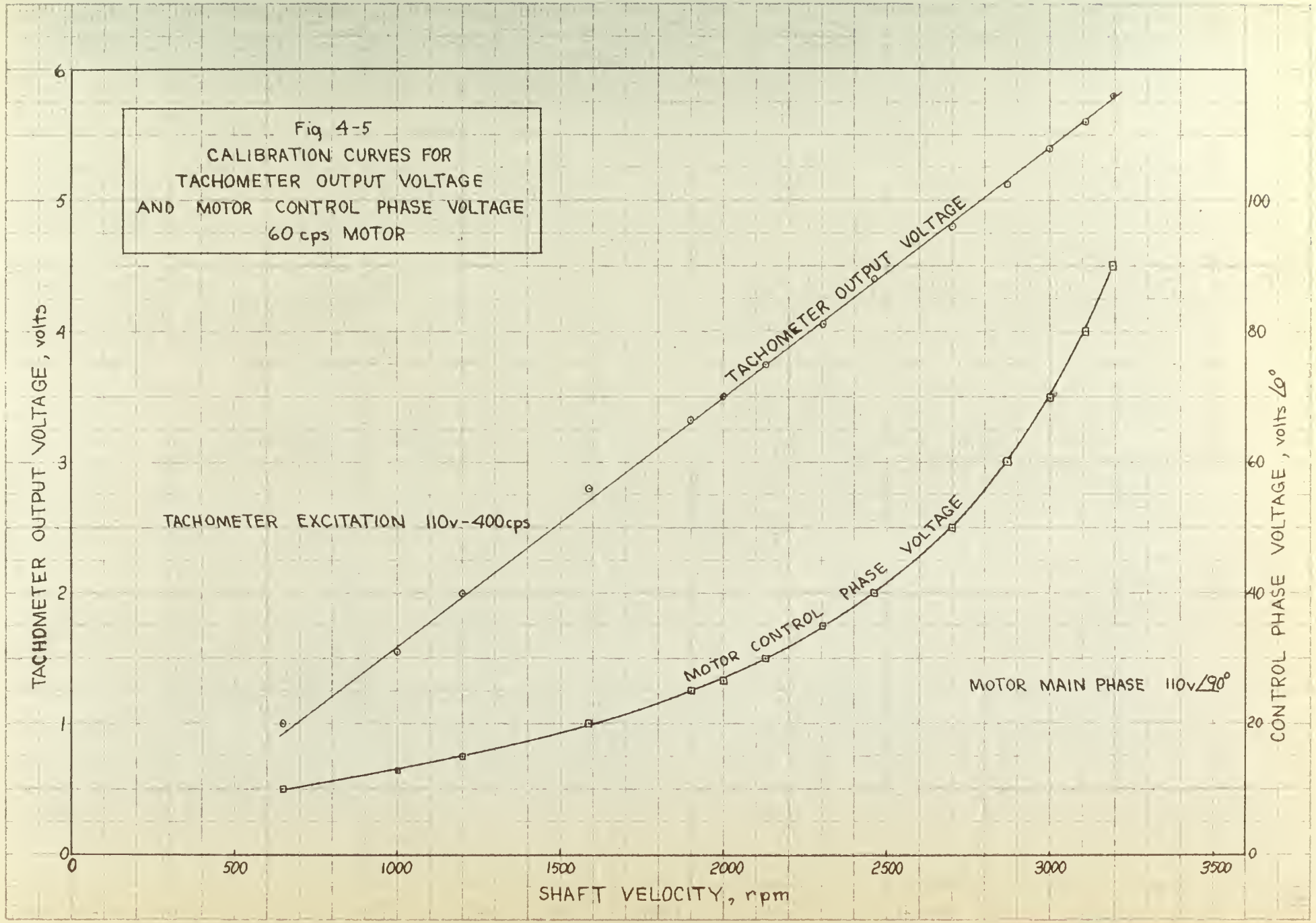
Fig 4-5
CALIBRATION CURVES FOR
TACHOMETER OUTPUT VOLTAGE
AND MOTOR CONTROL PHASE VOLTAGE
60 cps MOTOR
TACHOMETER OUTPUT VOLTAGE
MOTOR CONTROL PHASE VOLTAGE
TACHOMETER EXCITATION 110v-400cps
MOTOR MAIN PHASE 110v∠90°
TACHOMETER OUTPUT VOLTAGE, volts
CONTROL PHASE VOLTAGE, volts ∠0°
SHAFT VELOCITY, rpm
0
1
2
3
4
5
6
0
20
40
60
80
100
0
500
1000
1500
2000
2500
3000
3500

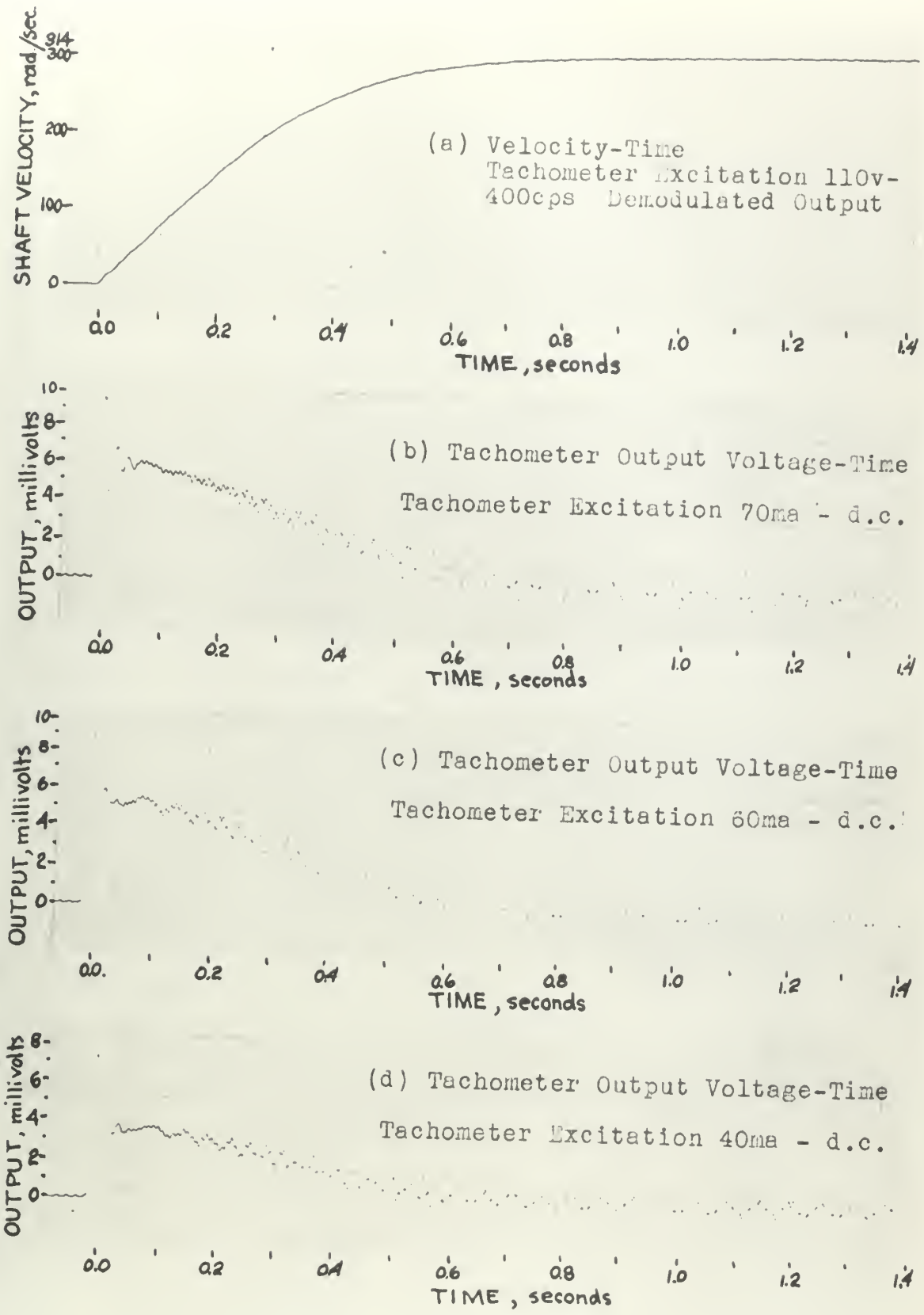

Fig. 4-6. Records of Exponential Motion Tests

speed was set by reading the output voltage of the a-c excited tachometer. Then the motor was shut off and the output of the a-c excited tachometer was fed, through a demodulator, into the recorder. When the motor was turned on, the demodulated tachometer output was recorded. This is shown on Fig. 4-6 (a). The maximum value of the curve corresponds to the steady state speed measured from the tachometer output voltage and the time constant is that time at which the curve has reached 63.2 percent of the steady state value.

After this speed curve was obtained, the excitation of the tachometer was changed to d-c and the potentiometer (Fig. 4-2), was adjusted to provide the excitation current desired. Using the same setting on the motor control phase voltage, and with the tachometer output fed directly into the recorder, the motor was again turned on and now a voltage output proportional to acceleration was obtained. Figs. 4-6 (b) through 4-6 (d), show this output voltage-time relationship.

The recorder was then voltage calibrated to obtain a scale for measuring the output voltage from the accelerometer (d-c excited tachometer).

There were oscillations present when the accelerometer output should have been at a steady state value of zero which would correspond to the steady state constant speed. An investigation of these oscillations led to changing from the 400 cps motor, with its common shaft and connecting iron

casing with the tachometer, to the use of a 60 cps motor, connected to the shaft extension of the 400 cps motor-tachometer unit. When the tachometer was not excited, but one of the 400 cps motor phases was excited, a study of the tachometer output revealed the presence of a 400 cps signal, even with the shaft stationary.

To eliminate this unwanted signal, the 60 cps motor was connected to the shaft and the 400 cps motor was left de-energized. Another unwanted signal was noted when the shaft was rotating at constant speed. The output was put on an oscilloscope and the signal was predominantly 800 cps when the 400 cps motor was used. It was decided that this signal was due to the normal double frequency torque variations of two phase induction motors. This was proved by observing the same condition when using the 60 cps motor. The predominant signal was now one of 120 cps, plus some higher order harmonics and also a signal of a lower frequency (approximately 45 cps). It was found that the lower frequency was reduced and the 120 cps signal made more predominant by changing the coupling from flexible rubber to a more rigid metal one. The increase in coupling rigidity had improved the reproduction of the torque variations of the motor and these torque variations produced detectable variations in angular acceleration. This detection of the motor torque variations proves the effectiveness of the device as an accelerometer.

Figs. 4-6 (a) through 4-6 (d) were made with the 60 cps motor driving the 400 cps motor and tachometer.

Sinusoidal Motion Tests

As stated previously, the sinusoidal motion was obtained by connecting the 400 cps motor shaft extension, directly onto the sinusoidal stroking attachment of the M.I.T. Servomechanisms Laboratory Sine-Drive (10).

Fig. 4-7 shows a sketch of the sinusoidal stroking attachment.

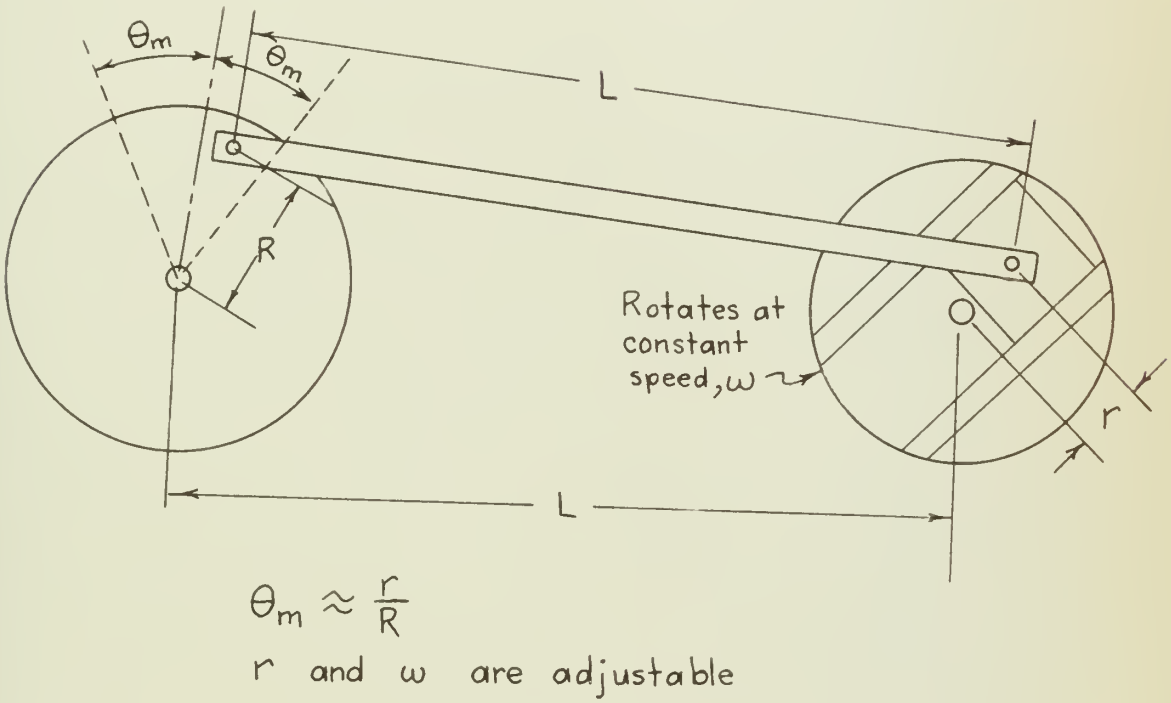

Fig. 4-7. Sinusoidal stroking attachment of sine-drive

This test consisted of measuring r and R to determine θ_m and then making various settings of the forcing frequency, ω, and then recording the accelerometer (d-c excited tachometer) output voltage. Fig. 4-8 is the result of a series of these tests.

When it became apparent that the curve was sloping upward with increasing forcing frequency, contrary to Eq.(27), the output was examined on an oscilloscope. It was found that the fundamental frequency approached a square wave with increasing frequency and became more sinusoidal at lower frequencies. The excitation on the tachometer was changed to 400 cps and now the output, which then represented shaft velocity, appeared on the oscilloscope as a 400 cps carrier, modulated with a triangular wave when the forcing frequency was high. This again confirms the fact that the tachometer, with d-c excitation is performing one more differentiation than it does with a-c excitation.

The detrimental effect of the square wave accelerometer output was that the output voltage readings were being made with a vacuum tube voltmeter which read the root mean square (rms) value, and this value changes with wave shape. Since the rms value of a wave increases as the wave shape goes from sinusoidal to square, this would explain the upward slope of the curve with increasing frequency, as shown on Fig. 4-8.

In general the testing mechanism is unsatisfactory for

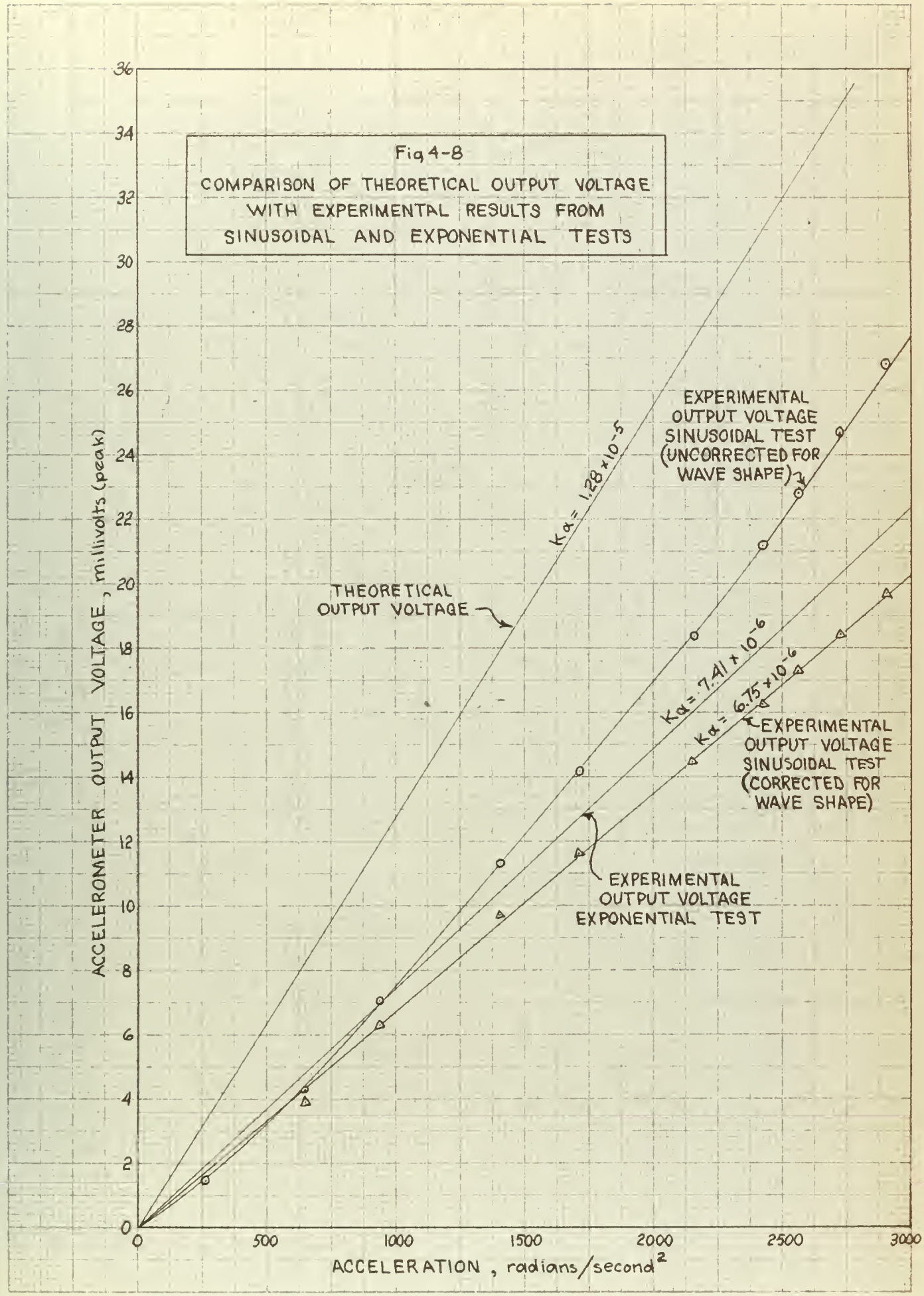
Fig 4-8
COMPARISON OF THEORETICAL OUTPUT VOLTAGE WITH EXPERIMENTAL RESULTS FROM SINUSOIDAL AND EXPONENTIAL TESTS
ACCELEROMETER OUTPUT VOLTAGE, millivolts (peak)
ACCELERATION, radians/second²
0
2
4
6
8
10
12
14
16
18
20
22
24
26
28
30
32
34
36
500
1000
1500
2000
2500
3000
THEORETICAL OUTPUT VOLTAGE
Kα = 1.28 x 10⁻⁵
EXPERIMENTAL OUTPUT VOLTAGE SINUSOIDAL TEST (UNCORRECTED FOR WAVE SHAPE)
Kα = 7.41 x 10⁻⁶
Kα = 6.75 x 10⁻⁶
EXPERIMENTAL OUTPUT VOLTAGE SINUSOIDAL TEST (CORRECTED FOR WAVE SHAPE)
EXPERIMENTAL OUTPUT VOLTAGE EXPONENTIAL TEST

this type of use, since the sine-drive itself is not designed to drive a large inertia (a tachometer drag-cup rotor plus the 400 cps motor rotor in our application) and the sine-drive is limited in frequency. The sine-drive does have a scotch-yoke attachment for driving heavier shafts but this attachment is limited to a frequency of 10 cps.

CHAPTER 5

DISCUSSION OF TEST RESULTS

Exponential Tests

A voltage output scale was made from the calibration of the Sanborn Recorder. This scale was used to pick off voltage values from the recorder tape representing acceleration for a particular time. The time scale was based on the 60 cps timing trace. Examples of the recorder tapes are shown on Fig. 4-6.

The values for velocity, $\dot{\theta}$, were taken from Fig. 4-6(a) and plotted on Fig. 4-3(a). The values for acceleration, $\ddot{\theta}$, as shown on Fig. 4-3(b), were obtained graphically from Fig. 4-3(a).

Using the values for $\dot{\theta}$ and $\ddot{\theta}$, and the values for e_{out} at selected time intervals, it was possible to solve for values of K/R and thus $K\alpha$, by trial solution of

$$e_{out} = K\alpha [DF]_{E2} \ddot{\theta}$$

$$e_{out} = \left(\frac{4\pi N_Y N_{mim}}{10^9 R}\right)\left(\frac{K}{R}\right)\left\{\frac{1-\left(\frac{K\dot{\theta}}{R}\right)^2}{\left[1+\left(\frac{K\dot{\theta}}{R}\right)^2\right]^2}\right\} \ddot{\theta}$$

The values of the other constants were obtained from Table 3-1.

By averaging the results from several values of time, the value of $K/R = 1.05 \times 10^{-3}$ was obtained. This value was used to compute a new $K\alpha$ which is now 7.42×10^{-6} volts/radian/second^2.

Fig. 5-1 shows the use of $[DF]_{E2}$, using the experimental

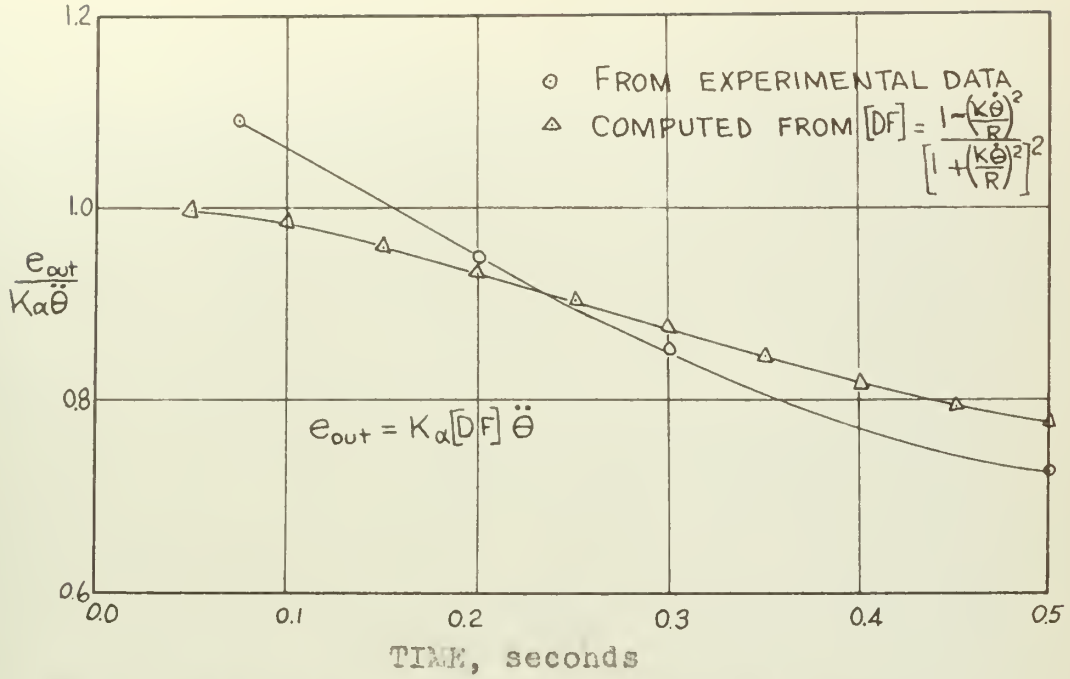

Fig. 5-1. Comparison of values of computed Deviation Function to experimentally determined values.

value of K/R, to compare with experimentally determined points.

Sinusoidal Tests

As previously stated in Chapter 4, the root-mean-square (rms) output increased with increasing forcing frequency, due to wave shape degeneration. Based on the observations of the wave shapes on an oscilloscope, the rms values of output voltage were corrected for wave shape. To make this correction for wave shape the frequency at which the output wave shape was sinusoidal, and that frequency at which the wave shape became square was determined. The rms values were corrected to peak values based on the assumption that the rms values for the changing wave shape increased linearly with frequency, up to the value for a

square wave. The effect of this correction is shown on Fig. 4-8.

After the wave shape correction was made, the slope of the voltage output vs $\ddot{\theta}$ curve of Fig. 4-8 provided the experimental determination of the Acceleration Proportionality Constant $K\alpha$.

Summary of Test Results

Both test methods provided an independent means of determining $K\alpha$. The results of the tests were

$$K\alpha = 7.42 \times 10^{-6} \text{ volts} \Big/ \frac{\text{radians}}{\text{second}^2} \quad \text{from exponential test}$$

$$K\alpha = 6.75 \times 10^{-6} \text{ volts} \Big/ \frac{\text{radians}}{\text{second}^2} \quad \text{from sinusoidal test}$$

Since these two values compare favorably, the value of K/R determined from the exponential test is considered as being correct. This value was $K/R = 1.05 \times 10^{-3}$ and is lower than the 1.81×10^{-3} that was predicted. The predicted value was based on the derivation of R in Appendix A. It is known that the derived value of R should be increased, since the derivation did not consider any resistance in the return paths between the two incremental coil sides (shown on Fig. A-1). An increase in the derived R will reduce the predicted K/R, bringing this ratio closer to the experimentally determined value.

CHAPTER 6

CONCLUSIONS AND RECOMMENDATIONS

Performance Equations

The comparison between the two experimentally determined Acceleration Proportionality Constants, K_α, verifies the analytical approach used in Chapter 2, if the value derived for R is modified as suggested in Chapter 5. This verifies the practicality of predicting the proportionality constant, to a reasonable degree of accuracy, from only the physical measurements.

The IBM Computer comparisons proved the accuracy of the assumptions used in the derivation of the Actual Performance Equations.

Therefore the Actual Performance Equation of a d-c excited, drag-cup, tachometer, is considered to be

$$e_{out} = K_\alpha [DF] \ddot{\theta}$$

where

$$[DF]_s = \frac{e^{-j\psi}}{\left[1+\left(\frac{L}{R}\right)^2\omega^2\right]^{1/2}} \qquad \text{for sinusoidal motion}$$

$$\psi = \tan^{-1}\frac{L\omega}{R}$$

ω = forcing frequency

or expressed in operator notation

$$[DF]_s = \frac{1}{T_\alpha p + 1} \qquad \text{a dynamic lag}$$

$$T_\alpha = \frac{L}{R}$$

$$[DF]_{E1} = 1 - e^{-\frac{R}{L}t} \qquad \text{for exponential motion } t < 0.03$$

$$[DF]_{E2} = \frac{1-\left(\frac{K\dot{\theta}}{R}\right)^2}{\left[1+\left(\frac{K\dot{\theta}}{R}\right)^2\right]^2} \qquad \text{for exponential motion } t > 0.03$$

For the AMA 15400, the K/R value has been changed, from that listed in Table 3-1, to the value 1.05×10^{-3} that was determined experimentally. The value of K/L is now 1815 and this gives a break point for $[DF]_s$ of 289 cps.

The above performance equations place limitations on the statement that the output voltage, of a d-c excited drag-cup tachometer, will be proportional to the shaft angular acceleration.

The normal use of this device in servo mechanisms, will be with sinusoidal shaft motion at frequencies where the Deviation Function has negligible effect. As the forcing frequency approaches the break point frequency, a phase lag will develop, which is in contrast to the effect noted by Fowle [5]. It is felt by the authors that Fowle, since he used a similar sine-drive, experienced the same wave shape degeneration with frequency, that the authors noted. This wave shape degeneration is discussed in Chapter 5.

Test Procedures

As previously stated in Chapter 4, the authors feel that a better method of sinusoidal shaft excitation is required if information is to be obtained above 20 cps. It is desirable to excite the shaft at higher frequencies to locate the break point frequency, and thus have an accurate means of determining K/L. Below 20 cps it is felt that the sinusoidal excitation provides an easy method

of obtaining the value of the Acceleration Proportionality Constant.

If the d-c excited tachometer is to be used as an accelerometer in a speed control mechanism, or in a manner that involves acceleration up to a constant speed, the exponential type test is recommended as the only method of determining the variation of the Deviation Function with shaft velocity.

It is felt that the Sanborn Recorder method of measuring the output voltage is adequate if a satisfactory preamplifier is available. In the exponential test method it is important to eliminate any source of shaft vibrations and it is advisable to use a d-c drive motor or possibly a drag-cup induction motor to eliminate the "cogging" effect of a wound rotor a-c induction motor.

The effect of shaft vibrations will be present regardless of the testing method used but is more apparent with the exponential test method.

Accelerometer Design Considerations

In any discussion of accelerometer design considerations it is necessary to examine the parameters that make up the Acceleration Proportionality Constant, K_α, and also the ratio R/L.

Neglecting all constants and considering only the parameters, K_α becomes,

$$K_\alpha = N_r N_m i_m \left(\frac{l}{R}\right)\left(\frac{K}{R}\right)$$

$$= N_r N_m i_m \left(\frac{r\ell}{g}\right)\left(\frac{ptr^2}{\rho g}\right)$$

$$\frac{R}{L} = \frac{\rho g}{ptr^2}$$

It is desirable to have R/L large to reduce the transient effect for the exponential motion and to increase the break point frequency for the sinusoidal motion. It is also desirable to have K/R large to increase the magnitude of the K_α. Examination reveals that both ratios contain the same parameters and an increase in a parameter will increase one ratio but decrease the other. Therefore any change of parameters that are mutual to R/L and K/R would have to be based on an optimization study of the performance equation for a particular use.

This leaves only the length of the pole face, the winding turns and the excitation current as parameters if optimization is not considered.

Any increase in the number of winding turns would involve a study of space, heat, wire size, excitation current and conductor resistivity.

If inertia is not critical, increasing the length of the pole face is an effective way to increase K_α.

APPENDIX A

DERIVATION OF EQUIVALENT ROTOR RESISTANCE*

The purpose of this derivation is to obtain a single turn rotor coil, with an equivalent resistance, which will produce the same mmf along the output axis as would be produced by the current sheet in the drag-cup.

Referring to Figs. A-1 and A-2:

$$d\lambda = NB\,dA$$

$$= B_m \ell r \left(\frac{2}{p}\right) d\theta_e \qquad \text{(A-1)}$$

where λ is the total number of flux lines linked by the single coil (N=1), and B_m is the flux density in gausses (lines per square centimeter). Since the area is expressed in electrical units, B_m has to be modified by the factor, 2/p, to take care of the difference between electrical degrees and mechanical degrees.

$$\lambda = \int_{\alpha}^{\pi+\alpha} B_m \ell r \left(\frac{2}{p}\right) d\theta_e$$

$$= \frac{2\pi}{p} B_m \ell r \qquad \text{lines} \qquad \text{(A-2)}$$

Since one coil links λ flux lines, the resulting distribution of lines is

$$\frac{\lambda}{\pi} = \frac{\text{lines}}{\text{radian}}$$

*This derivation is partially adapted from Fitzgerald and Kingsley (3).

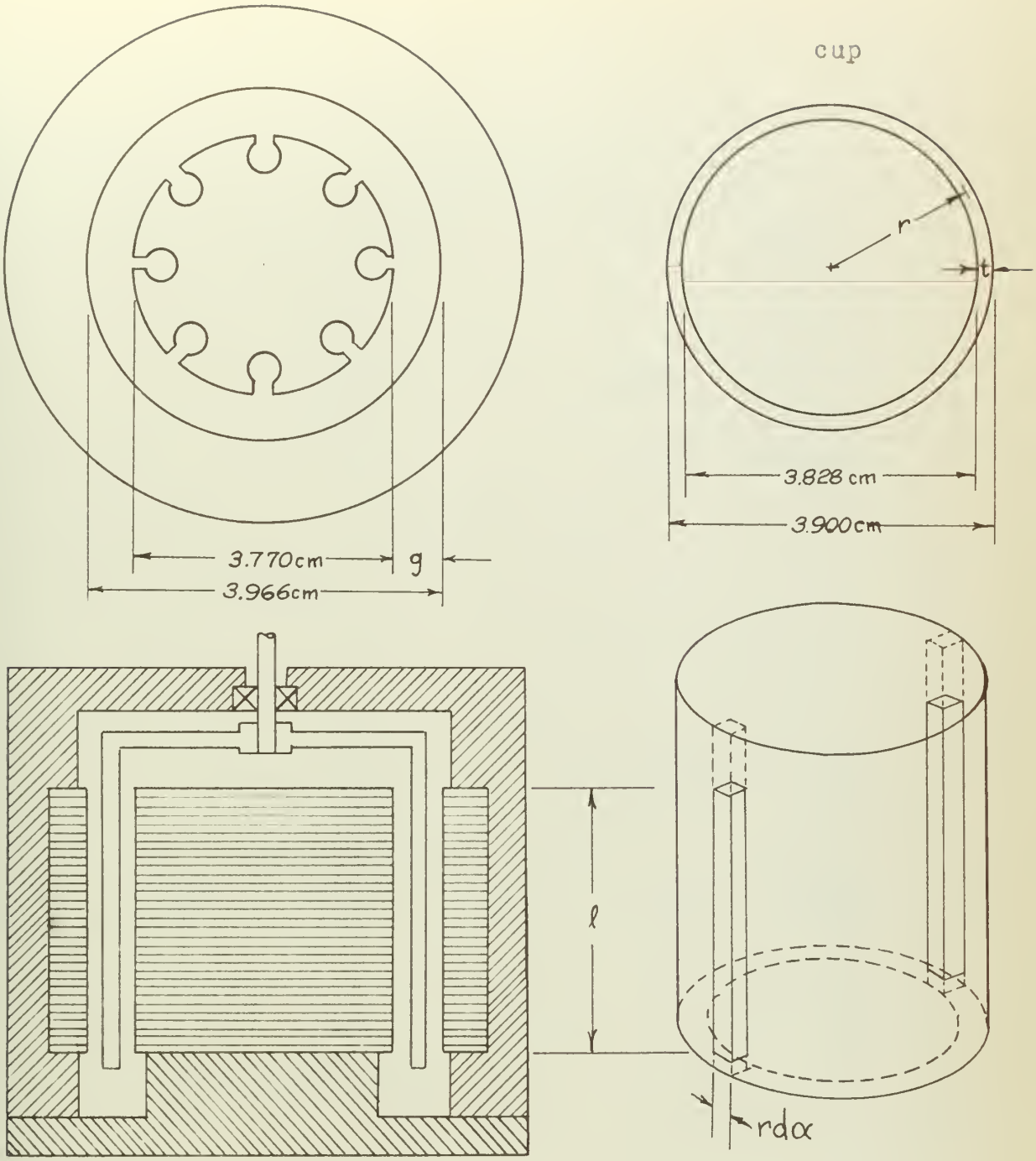

ε = 0.098 cm Resistivity of cup [8] = 14.9 μohms-cm
l = 2.163 cm
r = 1.934 cm
t = 0.036 cm

Main winding turns, N_m = 295
Quadrature winding turns, N_y = 406

Fig. A-1. Physical dimensions of an ARMA 1B400 INDUCTION GENERATOR

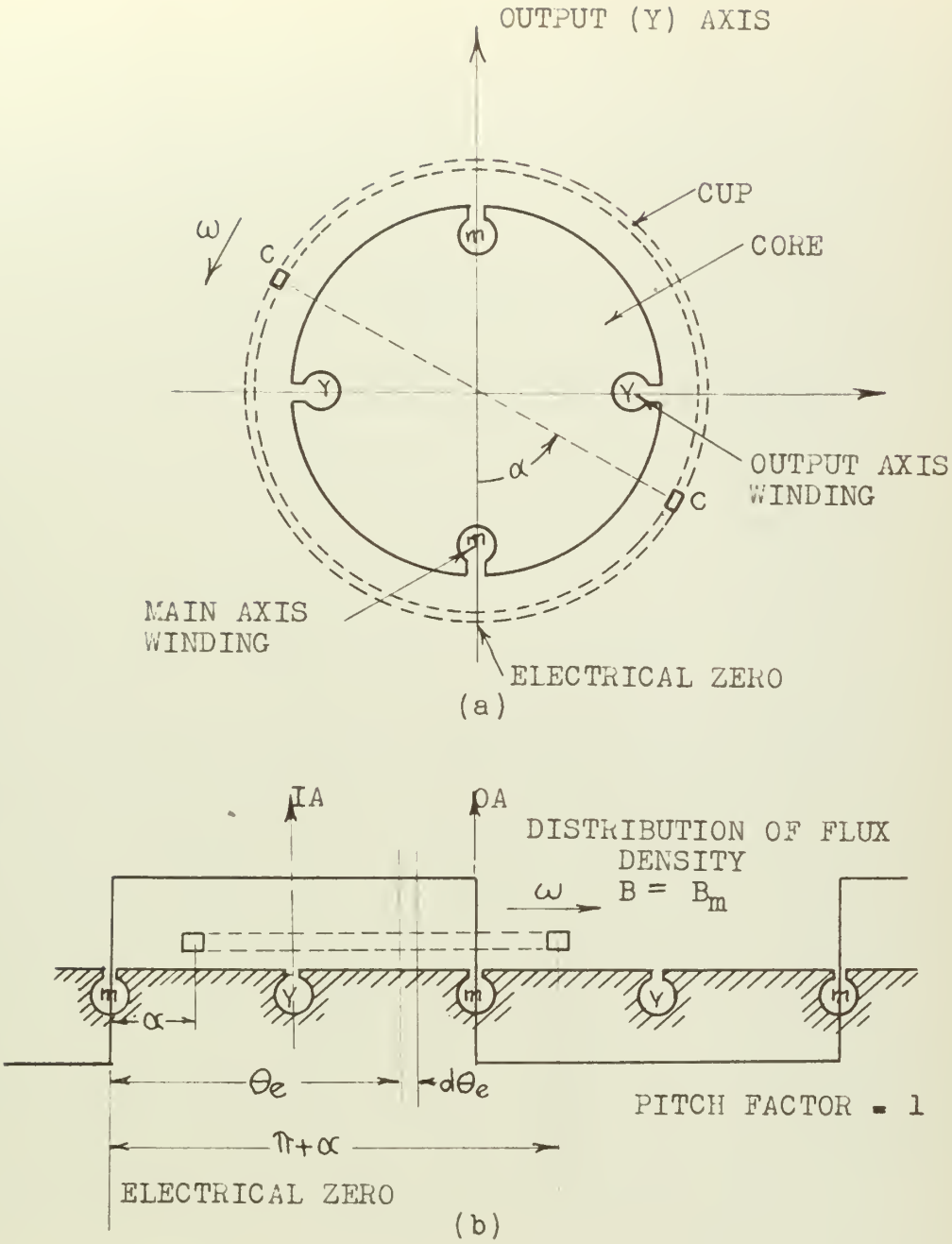

θ_e and α measured in electrical radians
ω in electrical radians/second
$\dot{\theta}$ in mechanical radians/second
B_g maximum flux density in gauss

Fig. A-2. (a) Single incremental rotor coil. (b) Diagram of a single coil in a rectangular flux distribution.

if each coil side is moving at ω electrical radians per second, and since

$$e_s = \frac{d\lambda}{dt}$$

$$e_s = \frac{2\lambda}{\pi}\omega = \frac{4B_m l r \omega}{p 10^8} \quad \text{volts} \qquad (A\text{-}3)$$

If mechanical radians are substituted for electrical

$$\omega = \frac{\dot{\theta} p}{2}$$

now

$$e_s = \frac{2}{10^8} B_m l r \dot{\theta} \quad \text{volts} \qquad (A\text{-}4)$$

This is still a general expression for a single incremental coil at position α. In this derivation the coil is considered to have only resistance, or for convenience, conductance. The conductance of one coil side* is

$$G = \frac{t r \, d\alpha}{\rho l} \quad \text{ohm}^{-1}$$

Since the coil consists of two of these increments in series and the conductance of the return paths in the cup are considered to have infinite conductance, then

$$G_c = \frac{t r \, d\alpha}{2\rho l} \quad \text{ohm}^{-1} \qquad (A\text{-}5)$$

This will be the conductance of one incremental coil regardless of the number of poles. The general expression

*Refer Fig. A-1

for the current in the incremental coil becomes

$$di_c = \left(\frac{p}{2}\right) e_s G_c$$

$$= \left(\frac{p}{2}\right)\left(\frac{1}{10^8} 2B_m \ell r\dot{\theta}\right)\left(\frac{trd\alpha}{2\rho\ell}\right) \quad \frac{\text{amperes}}{\text{radian}} \qquad (A\text{-}6)$$

The value of current in the incremental coil can also be considered the current density, in amperes per radians, of a current sheet of uniform current density as illustrated in Fig. A-3 (a).

The mmf acting on any path is equal to the total current enclosed by that path. If path A, Fig. A-3 (a), is chosen

$$\text{mmf} = \frac{1}{2}\left(\frac{4\pi}{10}\right)\int_{\pi}^{2\pi} di_c = \frac{1}{2}\left(\frac{4\pi}{10}\right) e_s \left(\frac{ptr}{4\rho\ell}\right)\int_{\pi}^{2\pi} d\alpha$$

$$= \frac{1}{2}\left(\frac{4\pi}{10}\right) e_s \left(\frac{ptr\pi}{4\rho\ell}\right) \quad \text{gilberts} \qquad (A\text{-}7)$$

The mmf magnitude is one half the total current since this current must force flux across two air gaps.

If path B, Fig. A-3 (b), is chosen, the net mmf is zero since the currents cancel out. The result is a mmf wave, as shown in Fig. A-3 (c), with a maximum value of

$$\frac{1}{2}\left(\frac{4\pi}{10}\right) e_s \left(\frac{ptr\pi}{4\rho\ell}\right)$$

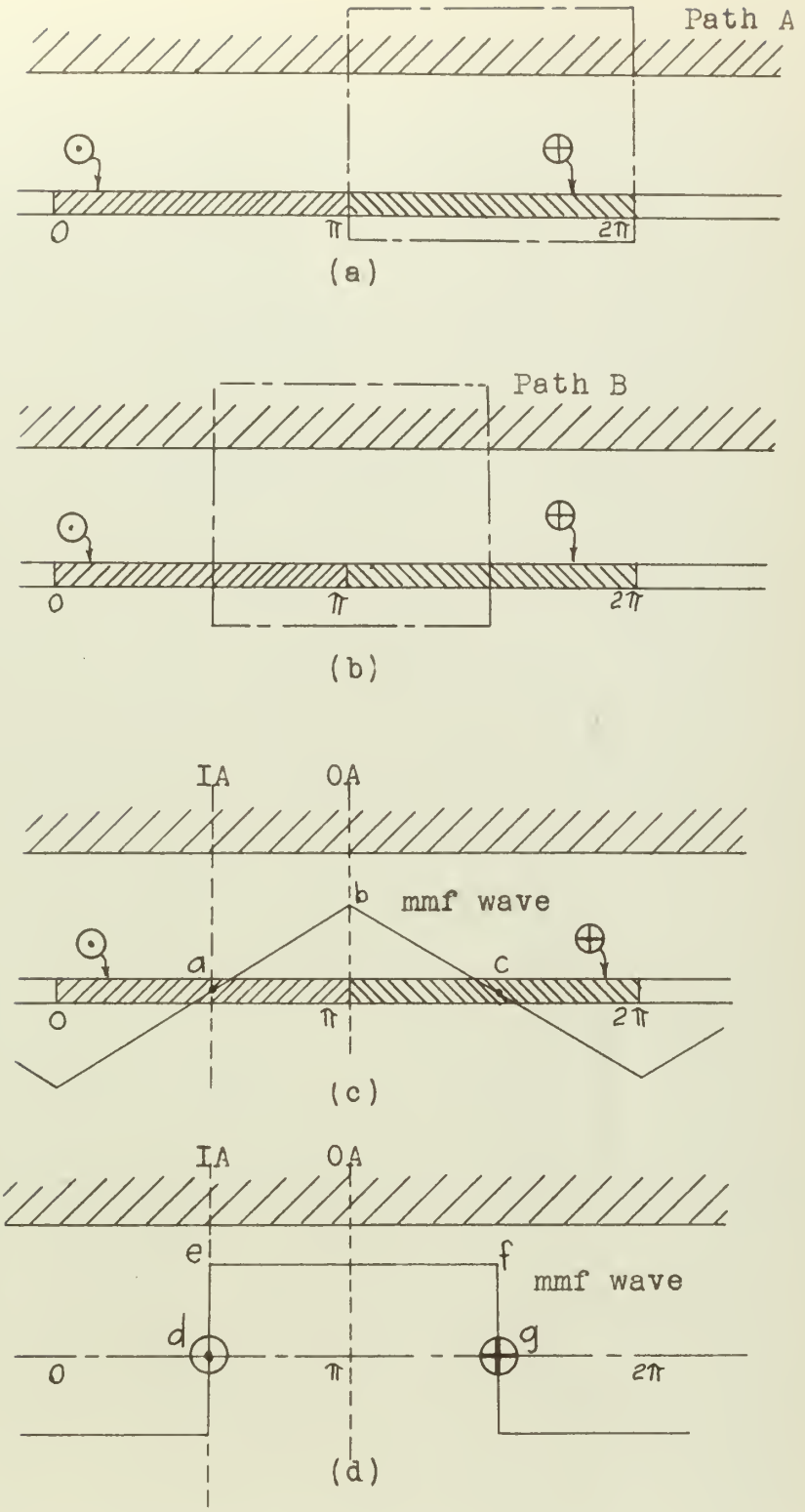

Fig. A-3. (a),(b) Uniform current sheet, mmf paths. (c) Mmf wave. (d) Equivalent coil mmf wave.

Fig. A-3 (d) represents a single coil that will produce the same mmf effect along the output axis (OA). For the effect of the single coil to be the same as for the current sheet, area abc must equal area defg. Therefore

$$X\pi = \frac{1}{2}\pi\left[\left(\frac{1}{2}\right)\left(\frac{4\pi}{10}\right)e_s\left(\frac{p\pi tr}{4\rho l}\right)\right]$$

$$X = \left(\frac{1}{2}\right)\left(\frac{4\pi}{10}\right)e_s\left(\frac{p\pi tr}{8\rho l}\right)$$

By equating out the similar terms in the expression above, it is possible to consider $\frac{8\rho l}{p\pi tr}$ as the equivalent resistance of the one turn coil of Fig. A-3 (d). This resistance will produce a current in this equivalent coil which in turn will produce the same mmf effect along the output axis.

Therefore

$$R = \frac{8\rho l}{p\pi tr} \quad \text{ohms} \qquad (A\text{-}6)$$

For the AMA 1B400 INDUCTION GENERATOR with 4 poles,

$R = \frac{2\rho l}{\pi tr}$ ohms. (A-7)

APPENDIX B

DERIVATION OF EQUIVALENT ROTOR INDUCTANCE

The purpose of this derivation is to obtain a value of inductance for a single turn coil that is equivalent to the inductance of the entire cup.

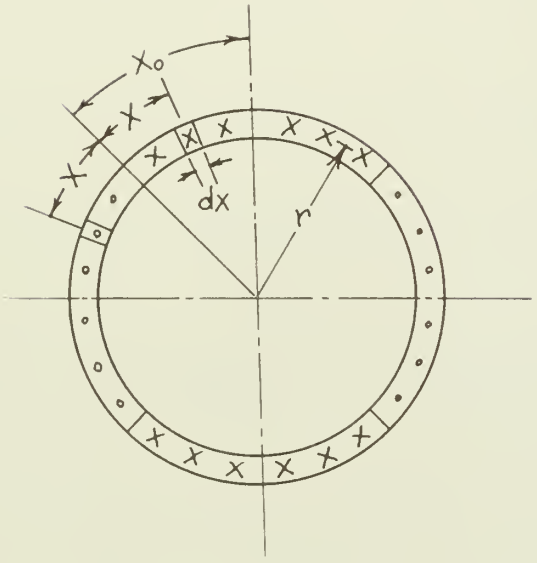

Fig. B-1. Current distribution in the drag-cup

The derivation assumes that the current is uniformly distributed over four quadrants (four pole machine), with the directions of flow as shown in Fig. B-1. The actual space orientation of these quadrants depends upon the orientation of the resultant rotor flux at any particular instant of time.

Each quadrant is considered to be a flat plate in an air gap, as shown in Fig. B-2.

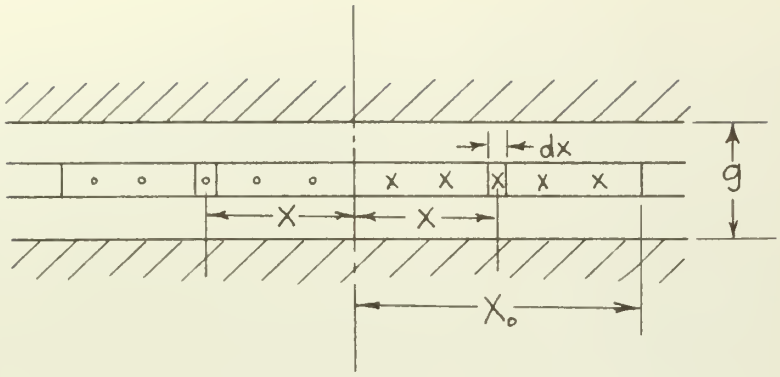

(Fig. B-2. Flat plate representation of a drag-cup quadrant)

The flux produced by the incremental turn, with sides at X, is

$$d\phi = \frac{4\pi}{10} \frac{N dI}{\mathcal{R}} \qquad \text{lines (maxwells)} \quad \text{(B-1)}$$

where

$$\mathcal{R} = \frac{(gap)}{area} = \frac{g}{2lr} \qquad \text{cm}^{-1}$$

and l is the axial length of the pole face, g is the length of the air gap, and dI is the current (in amperes) per radian or the current in the incremental coil. The flux per pair of poles is also $d\phi$ since for a pair of poles there would be 2dI and 2g.

The number of flux linkages, $d\lambda$, with the electric circuit (per pair of poles) is

$$d\lambda = d\phi \frac{X_o - X}{X_o}$$

$$= \left(\frac{4\pi dI}{10}\right)\left(\frac{2l}{g}\right)\left(\frac{X_o X - X^2}{X_o}\right) \qquad \text{lines}$$

or since

$$dI = I\frac{dx}{X_o} \qquad \text{amperes}$$

then

$$d\lambda = \left(\frac{4\pi}{10}\right)\left(\frac{2\ell I}{q}\right)\left(\frac{X_o X - X^2}{X_o^2}\right)dx \qquad \text{lines} \qquad (B\text{-}2)$$

where I is the total current in the cup under a pair of poles, and is assumed to be uniformly distributed over the cross-sectional area. Therefore the total linkages, per pair of poles, is

$$\lambda = \int_o^{X_o}\left(\frac{4\pi}{10}\right)\left(\frac{2\ell I}{q}\right)\left(\frac{X_o X - X^2}{X_o^2}\right)dx$$

$$= \left(\frac{4\pi}{10}\right)\left(\frac{2\ell I}{q}\right)\left(\frac{X_o}{6}\right)$$

$$= \left(\frac{4\pi}{10}\right)\left(\frac{\ell I X_o}{3q}\right) \qquad \text{lines} \qquad (B\text{-}3)$$

The inductance, per pair of poles, can now be expressed as

$$L = \frac{\lambda}{I} \qquad \frac{\text{weber-turns}}{\text{ampere}} \text{ or henrys}$$

$$= \frac{4\pi\ell X_o}{3q} \times 10^{-9} \qquad \text{henrys} \qquad (B\text{-}4)$$

and

$$X_o = \frac{2\pi r}{2p} = \frac{\pi r}{p}$$

where p is the number of poles of the device. The inductance now becomes

$$L = \frac{4\pi^2 r \ell}{3qp} \times 10^{-9} \quad \text{henrys/pair of poles} \qquad (B\text{-}5)$$

Using the measurements of the AMA 1B400 INDUCTION GENERATOR from Table 3-1, the value for L (considering two pairs of poles) becomes

$$L = (2)\frac{4\pi^2 r \ell}{3q(4)} \times 10^{-9}$$

$$= \frac{2\pi^2 (2.163)(1.934)}{3(0.0982)}$$

$$= \underline{\underline{2.80 \times 10^{-7}}} \quad \text{henrys} \qquad (B\text{-}6)$$

APPENDIX C

BIBLIOGRAPHY

1. W. R. Ahrendt: Servomechanism Practice, McGraw-Hill Book Company, Inc., New York, N. Y., 1954

2. E. Davis: "Rotating Components for Automatic Control", Product Engineering, Vol. 24, November 1953.

3. A. E. Fitzgerald and C. Kingsley, Jr.: Electric Machinery, McGraw-Hill Book Company, Inc., New York, N. Y., 1952

4. R. S. Lovett: Improving Dynamic Response of Servomechanisms By Second Derivative Feedback, Master of Science Thesis, Massachusetts Institute of Technology, EE Dept., 1950

5. E. W. Fowle: Acceleration-Stabilized, Positional Servomechanism Employing a Two-Phase Induction Motor, Master of Science Thesis, Massachusetts Institute of Technology, EE Dept. 1957

6. W. W. Eshbach: Handbook of Engineering Fundamentals, John Wiley & Sons, Inc., New York, N. Y., 2nd Edition

7. R. M. Frazier: Analysis of Drag-Cup A-C Tachometer by Means of Two-Phase Symmetrical Components, Dynamic Analysis and Control Laboratory M.I.T. Memorandum, DSR-4.10-4, May 15, 1950, Cambridge, Mass., 1950

8. R. M. Frazier: Measurements Made on Cup and Core Material of AMF Type 1B400 Tachometer, Dynamic Analysis and Control Laboratory M.I.T. Memorandum, DSR-4.0-50, April 30, 1952, Cambridge, Mass., 1952

9. M. F. Gardner and J. L. Barnes: Transients in Linear Systems, Volume I, John Wiley & Sons, Inc., New York, N.Y., 1942

10. G. A. Bernsen: Theory and Operation of the M.I.T. Servomechanisms Laboratory Sine Drive, Eng. Report 254, Servomechanisms Laboratory, M.I.T., Cambridge, Mass., November 30, 1951